



1 Greenhouse gas emissions and their trends over the last three decades across 2 Africa

3 Mounia Mostefaoui¹, Philippe Ciais², Matthew J. McGrath², Philippe Peylin², Prabir K.
4 Patra³, Yolandi Ernst⁴

5 ¹Laboratoire de Météorologie Dynamique/IPSL, École Normale Supérieure, PSL Research University,
6 Sorbonne University, École Polytechnique, IP Paris, CNRS, Paris, France.

7 ²Laboratoire des Sciences du Climat et de l'Environnement, 91190 Gif-sur-Yvette, France.

8 ³Research Institute for Global Change, JAMSTEC, Yokohama 2360001, Japan.

9 ⁴Global Change Institute, University of the Witwatersrand, Johannesburg, South Africa.

10 *Correspondence to:* mounia.mostefaoui@polytechnique.edu

11 **Key words:** greenhouse gasses, anthropogenic emissions and removals, fossil fuels, land-use, land-use change and
12 forestry, Africa, bottom-up, top-down atmospheric inversions, UNFCCC inventories, Global Carbon Project,
13 PRIMAP-hist, IPCC sectors, climate change, Paris Agreement, Global Stocktake, Monitoring, Reporting and
14 Verification.

15 **Abstract.** A key goal of the Paris Agreement (PA) is to reach net-zero Greenhouse Gasses (GHG) emissions by 2050
16 globally, which requires mitigation efforts from all countries. Africa's rapidly growing population and GDP makes
17 this continent important for GHG emission trends. In this paper, we study the emissions of carbon dioxide (CO₂),
18 methane (CH₄) and nitrous oxide (N₂O) in Africa over three decades (1990-2018). We compare bottom-up approaches
19 including UNFCCC national inventories, FAO, PRIMAP-hist, process-based ecosystem models for CO₂ fluxes in the
20 Land Use, Land Use Change and Forestry (LULUCF) sector, and global atmospheric inversions. Our database is
21 available from Zenodo at: <https://doi.org/10.5281/zenodo.7347077> (Mostefaoui et al., 2022). For inversions, we
22 applied different methods to separate anthropogenic CH₄ emissions. The bottom-up (BU) inventories show that over
23 the decade 2010-2018, less than ten countries represented more than 75% of African fossil CO₂ emissions. With a
24 mean of 1373 MtCO₂ yr⁻¹, total African fossil CO₂ emissions over 2010-2018 represent only 4% of global fossil
25 emissions. Yet, these emissions grew by +34% from 1990-1999 to 2000-2009 and by +31% over 2000-2009 to 2010-
26 2018, more than doubling in 30 years. This growth rate is more than twice faster than the global growth rate of fossil
27 CO₂ emissions. The anthropogenic emissions of CH₄ grew by 5% from 1990-1999 to 2000-2009 and by 14.8% from
28 2000-2009 to 2010-2018. The N₂O emissions grew by 19.5% from 1990-1999 to 2000-2009; and by 20.8% from
29 2000-2009 to 2010-2018. When using the mean of estimates from UNFCCC reports (including the land use sector),
30 with corrections from outliers, Africa was a mean source of greenhouse gasses of +2622³²³⁹₂₁₈₆ MtCO₂e yr⁻¹ from all
31 bottom-up estimates (sub- and superscript indicating min-max range uncertainties), and of +2637⁵⁸⁷³₁₇₆₁ MtCO₂e yr⁻¹
32 from top-down methods, during their overlap period from 2001 to 2017. Although the mean values are consistent, the
33 range of top-down estimates is larger than the one of bottom up, indicating that sparse atmospheric observations and
34 transport model errors do not allow us to use inversions to reduce the uncertainty of bottom-up estimates. A main
35 source of uncertainty comes from CO₂ fluxes in the land-use sector (LULUCF) for which the spread across inversions
36 is larger than 50%, especially in Central Africa. Moreover, estimates from national UNFCCC communications differ



37 widely depending on whether the large sinks in a few countries are corrected to more plausible values using more
38 recent national sources following the methodology of Grassi et al. (2022) The median of CH₄ emissions from
39 inversions based on satellite retrievals and in situ surface networks are consistent with each other within 2% at
40 continental scale. The inversion ensemble also provides consistent estimates of anthropogenic CH₄ emissions with
41 bottom-up inventories such as PRIMAP-hist. For N₂O, inversions systematically show higher emissions than
42 inventories, on average about 4.5 times more than PRIMAP-hist, either because natural N₂O sources cannot be
43 separated accurately from anthropogenic ones in inversions, or because bottom-up estimates ignore indirect emissions
44 and under-estimate emission factors. Future improvements can be expected thanks to a denser network for monitoring
45 atmospheric concentrations. This study helps to introduce methods to enhance the scope of use of various published
46 datasets and allows to compute budgets thanks to recombinations those data products. Our results allow to understand
47 uncertainty and trends of emissions and removals in a region of the world where few observations exist and most
48 inventories are based on default IPCC guidelines values. The results can therefore serve as a support tool for the Global
49 Stocktake (GST) of the Paris Agreement. The referenced datasets related to figures are available at:
50 <https://doi.org/10.5281/zenodo.7347077> (Mostefaoui et al., 2022).



51 **Introduction**

52 Large global reductions of greenhouse gasses (GHG) emissions are needed to avoid “dangerous
53 anthropogenic interference with the climate system” (IPCC, 2021). The Paris Agreement (PA) aims at
54 limiting global warming below 2°C and reaching “net-zero GHG emissions by 2050” (UNFCCC,
55 2015). To improve the monitoring of emissions trends, the PA has an Enhanced Transparency
56 Framework (ETF) by which countries will have to report their GHG emissions and removals under a
57 standardized format starting in 2024 (Perugini et al., 2021; UNFCCC, 2021) through Biennial
58 Transparency Reports (BTR), with the ambition to use up-to-date data and best available science to
59 improve national inventories. This represents a challenge for many developing countries, where
60 emissions inventories have been irregular.

61 Recent analyses predict a fast increase of African emissions correlated with demographic growth. The
62 African population is expected to double from 1.2 billion in 2019 to 2.5 billion at the 2050 horizon
63 (UN, 2019). Using the TIAM-ECN Integrated Assessment Model (IAM) developed with data from the
64 International Energy Agency (IEA), van der Zwaan et al., (2018) concluded that greenhouse gasses
65 (GHG) emissions from Africa will become substantial at the global scale by 2050. In Shared Socio-
66 economic Pathways (SSP) projection scenarios, Africa and the Middle East are grouped together
67 despite having very different geographies, per capita emissions and Gross Domestic Product (GDP)
68 (IIASA, 2017). According to IAM projections, the minimum projected share of Africa in global
69 emissions would be close to 10% by 2050 for a business-as-usual pathway. An “explosive growth in
70 African combustion emissions” (Lioussé et al., 2014) could not be excluded from 2030 to 2050, if no
71 drastic mitigation policies are implemented (IPCC, 2021). If a stringent emissions reduction pathway
72 limiting global warming to +2 °C is adopted, Africa could contribute to around 20% of global emissions
73 by 2050, becoming the second largest worldwide emitting region. Further, under stringent climate
74 policy scenarios, CH₄ and N₂O emissions in Africa were projected to contribute 80% of the total
75 emissions of these two gasses in 2050 (van der Zwaan et al., 2018). Therefore, Africa will become an
76 important global emission contributor under any mitigation pathway with a demographical and
77 industrial development increase.

78 There are 56 African countries represented in the United Nations. National emissions reports to the
79 United Nations Convention Framework on Climate Change (UNFCCC) are available for 53 countries,
80 including all major African emitters. Africa as a whole ranks fifth worldwide in terms of territorial
81 fossil fuels use with a total of 1449 MtCO_{2e}, in-between the Russian Federation and Japan
82 (Friedlingstein et al., 2020). The global share of Africa is ~4% of fossil CO₂ (FCO₂) emissions, ~16



83 % of CH₄ emissions (Saunois et al., 2020) and ~25% of N₂O emissions (Tian, 2020). South Africa is
84 the biggest FCO₂ emitter in the continent, and ranked twelve on the global scale, just after Brazil.
85 Despite projections of strong growth of emissions and population in Africa, the continent is under-
86 studied and lacks up-to-date comprehensive assessments of GHG emissions and removals, given
87 sporadic and often outdated reports by individual countries. The literature tends to be scarce about
88 African countries, and their emissions have rarely been analyzed comprehensively using the results
89 from both statistical inventories that are also referred to as bottom-up (BU) methods, and from top-
90 down (TD) atmospheric inversions. Inversions results are uncertain due to the small number of
91 atmospheric stations over the continent (Nickless et al., 2020). A previous analysis of African emissions
92 was solely focused on FCO₂ emissions during the decade 2000-2009 (Canadell et al., 2009). A first
93 budget for the period 1990-2009 was provided at the continental scale with the RECCAP1 project
94 (Valentini et al., 2014). Ayompe et al. (2020) studied recent FCO₂ emissions trends, using International
95 Energy Agency (IEA) data. Other studies are region-specific or sector-specific, focusing exclusively
96 on agriculture (Bombelli et al., 2009), on natural ecosystems in Sub-Saharan Africa (Kim et al., 2016)
97 or in individual countries such as Kenya (Zhu et al., 2018).
98 Paying attention not only to commonly identified big emitters like South Africa, but also to medium
99 emitters and to emerging emitters is important, not only in terms of scientific assessment, but also for
100 financial and climate policy purposes under the PA. The Monitoring, Reporting and Verification
101 (MRV) provisions of the PA indeed require scientific and policy tools to verify the pledges made by
102 all the signatory countries. Instruments for financial transfers for mitigation and adaptation like the
103 Green Fund on Climate Change (GCF) and the REDD+ initiatives cover the African scope and will
104 require scientific assessment of trends for impact evaluation and credibility purposes, and as an
105 incentive for continued investments. As part of the Global Stock Take (GST) under article 14 of the
106 PA aiming at assessing “collective progress”, all signatory parties will have to show their contributions
107 to the global mitigation efforts. These efforts will be evaluated within a MRV system which includes
108 the requirement for developing countries to submit their Biennial Update Reports (BUR) on a biennial
109 basis starting in 2024. As no standard global reporting framework has been required to date, we
110 anticipate that the data available for the first stocktake in 2023 will be very heterogeneous. As a
111 continent gathering non-Annex I countries exclusively, the African case is featured by the scarcity of
112 national official inventories which have been provided to date on a voluntary basis through National
113 Communication (NC) and BUR. BU estimates of emissions established by independent scientific
114 methods are also discussed in the present study. In this context, different and complementary
115 observation-based methods assessing national GHG emissions and sinks are needed.



116 The aim of this paper is to evaluate relative merits of different existing types of datasets for the
117 assessment of African emissions and removals and their trends for CO₂, CH₄ and N₂O during the last
118 three decades. In this paper, we standardize the metrics and scope of application for different categories
119 of GHG emissions to discuss budgets. We also validate and benchmark different independent datasets
120 to evaluate the possibility to use them as a verifying tool for official country-reported data. In order to
121 cover all GHG sectors, we also describe recombinations of different historical datasets for the last 30
122 years that are necessary to fill the gap for some missing past sectorial emissions. This study offers a
123 comparison of data products originally combined to compute a budget and an evaluation of their
124 relative merits. The different data products discussed here include different bottom-up (BU)
125 approaches, including official countries communications to the UNFCCC and estimations from the
126 Food and Agriculture Organization (FAO), Carbon Dioxide Information Analysis Center (CDIAC),
127 global inventories for anthropogenic emissions (PRIMAP-hist which integrates combinations of
128 various datasets including FAO and Global Carbon Project (GCP)), and process-based models for land
129 CO₂ fluxes with 14 Dynamic General Vegetation Models (DGVM) from the TRENDY version 9
130 ensemble (Table 1). We also analyze and combine top-down data products to discuss individual gas
131 and to compute budgets: three atmospheric global inversions for CO₂ land fluxes; 22 inversions for
132 CH₄ emissions (11 in situ inversion models and 11 satellite inversion models) and CH₄ wildfire
133 emissions from the Global Fires Emission Dataset (GFED) version 4. We used three inversion models
134 for N₂O fluxes (PyVAR model, TOMCAT-INVICAT model, and MIROC4-ACTM model (see Table
135 1). Inversions only solve for total fluxes or at best for groups of sectors, whereas BU estimates have a
136 larger number of sectors. In Table 2, we present the correspondence between ‘sectors’ defined by the
137 TD and BU methods. For all datasets, we chose an atmospheric convention with negative values
138 representing removals from the atmosphere (i.e. land sink). We deliver an original comparison of BU
139 estimates from national inventories, global inventories, and process-based models, with TD estimates
140 from atmospheric inversions over Africa. The work is carried out for large countries or groups of small
141 countries, as inversions do not have the capability to constrain fluxes over small areas given their coarse
142 grid and sparse atmospheric data. Based on the benchmarking and relative merits evaluation of the
143 various data products presented above, the scientific questions addressed in this study are: 1) How
144 consistent are the mean values and trends of GHG emissions across BU estimates in Africa? 2) How
145 consistent are the different inversion model results? 3) How do inversions compare with bottom-up
146 estimates? 4) What is the net GHG balance of the African continent from different observation-based
147 methods, including CO₂ sinks and sources in the land-use sector? 5) What are the main sources of
148 uncertainties?



149 The manuscript is organized into two main sections. First, a material and methods section describes the
150 regional breakdown and input data (section 1). We present our results for the whole Africa and for six
151 groups of aggregated countries (section 2) with a specific analysis of CO₂ emissions and sinks, divided
152 between FCO₂ (section 2.1), fluxes in the land use, land use change and forestry (LULUCF) sector
153 (section 2.2), and emissions of non-CO₂ greenhouse gasses (sections 2.3 and 2.4). Conclusions are
154 drawn about uncertainties of African GHG net emissions and removals assessment.

155 **1 Methods and datasets**

156 This study covers the period from 1990 to 2018, and emissions and sinks of CO₂, CH₄ and N₂O. We
157 used 1990 as a base year since reporting to the UNFCCC mostly started in that year and is often used
158 as a reference comparison year in national pledges of the PA. The last year of analysis is 2018,
159 reflecting the availability of inversion data and avoiding further uncertainty due to poorly understood
160 emissions changes before and after the COVID19 crisis. This period allows the analysis of decadal
161 features. It also has the advantage of being covered by several datasets, listed in Table 1. We considered
162 different bottom-up (BU) approaches, including official countries communications to the UNFCCC
163 and estimations from the Food and Agriculture Organization (FAO), global inventories for
164 anthropogenic emissions (PRIMAP-hist which integrates combinations of various datasets including
165 FAO, GCP, EDGAR v4.3.2, Andrew 2018 cement data, Biennial Updaed Reports (BUR), Common
166 Reporting Format (CRF), UNFCCC data, and BP), and process-based models for land CO₂ fluxes with
167 14 Dynamic General Vegetation Models (DGVM) from the TRENDY version 9 ensemble (Table 1).
168 We used three atmospheric global inversions for CO₂ land fluxes; 22 inversions for CH₄ emissions;
169 and three inversions for N₂O fluxes (Table 1). Inversions only solve for total fluxes or at best for groups
170 of sectors, whereas BU estimates have a larger number of sectors. In Table 2, we present the
171 correspondence between ‘sectors’ defined by the TD and BU methods. For all datasets, we chose an
172 atmospheric convention with negative values representing removals from the atmosphere (i.e. land
173 sink). No specific standard guidelines currently exist for defining uncertainties for datasets from BU
174 and TD data products. In general, uncertainty estimates are understood as the spread among minimum
175 and maximum values from one methodology. A main source of uncertainty in the comparison of
176 country-reported data with other data products is the inclusion or not of natural fluxes additionally to
177 anthropogenic emissions sectors. For inversions, the prior geospatial distribution of emissions is a
178 critical source of uncertainty. For the comparability of the different data products presented in this
179 study, we discuss only the mean value over the period of overlapping data availability. Referenced
180 datasets are available at <https://doi.org/10.5281/zenodo.7347077>(Mostefaoui et al., 2022).



181
 182
 183

Table 1. List of BU and TD methods used. (For more details, see also Saunio et al. (2020) for CH₄, Friedlingstein et al. (2020) for FCO₂; UNFCCC country-reported data; Gütschow et al. (2021) for PRIMAP-hist).

Dataset name	Method	CO ₂	CH ₄	N ₂ O	Spatial resolution (longitude × latitude)	Time period covered in the present work
Inversions						
Global Carbon Budget ensemble (2020)	TD	×			from 1° × 1° to 6° × 4°	2000-2019
Global Methane Budget ensemble⁽¹⁾ (2020)	TD		×		from 1° × 1° to 6° × 4°	2000-2017 ⁽²⁾
PyVAR	TD			×	3.75° × 1.875°	1998-2017
TOMCAT-INVICAT	TD			×	5.6° × 5.6°	1998-2015
MIROC4 -ACTM	TD			×	2.8° × 2.8°	1998-2016
DGVMs						
TRENDYv9⁽³⁾	BU				0.5° × 0.5° (land surface) or 1° × 1°	1990-2019
Other BU inventories						
PRIMAP-hist (excluding LULUCF)	BU	×	×	×	country	1990-2019
GCB (CDIAC) (excluding LULUCF)	BU	×			0.1° × 0.1°	1990-2019
UNFCCC	BU	×			country	1990-2015
FAO (LULUCF CO ₂)	BU	×			country	1990-2019
GFEDv4 (wildfires only)	BU		×		0.25° × 0.25°	1997–2016

184
 185
 186
 187

⁽¹⁾ See 22 inversions details in the supplementary Table S6.

⁽²⁾ Variations from 2003-2015, 2000-2015, 2010-2017: see detailed period coverage for each dataset in the supplementary Table S6.

⁽³⁾ See supplementary Table S5 for the 14 products



188 **Table 2. Sectoral reconciliation between categories defined in TD and BU methods.**

Gas	Sector label choice for BU and TD	TD inversions	BU inventories
CO ₂	Net land flux	Total Net Biome Productivity (NBP) after subtraction of prior prescribed Fossil CO ₂	Energy + Industrial Processes and Product Use + Agriculture + Waste + Biomass burning
CH ₄	Total anthropogenic emissions	Fossil + Anthropogenic Biomass burning (BBUR) + Agriculture & Waste -Wildfires	Energy + Industrial Processes + Agriculture +Waste + Biomass burning
N ₂ O	Total	Total	All IPCC sectors

189 **1.1 Regional breakdown**

190 As some countries are small emitters and their area is too small to be resolved by inversions, and in some
 191 cases even by DGVMs, we grouped African countries into six regions shown in Figure S1 and listed in
 192 Table S1. The grouping followed national borders and biomes similarity considering the Köppen-Geiger
 193 climate zones (Beck et al., 2018), magnitudes of fossil fuel emissions, and per capita emissions (Fig. S1,
 194 Fig. S2 and Fig. S7). We also grouped a maximum of about ten countries per region.

195 **1.2 Inventories**

196 **PRIMAP-hist anthropogenic emissions assessment for CO₂, CH₄, and N₂O**

197 The PRIMAP-hist version 2.2 BU dataset is derived from Gütschow et al., (2021) and combines UNFCCC
 198 reports with a gap-filling method to produce a time series of annual anthropogenic emissions for different
 199 IPCC sectors. PRIMAP-hist does not cover the LULUCF sector for CO₂ due to the high uncertainties.
 200 PRIMAP-hist does not include emissions from shipping and international aviation, but includes cement as
 201 part of FCO₂ emissions. We use data from the HISTCR scenario (data accessed from [https://www.pik-
 202 potsdam.de/paris-reality-check/primap-hist/](https://www.pik-potsdam.de/paris-reality-check/primap-hist/) in April 2022) from country-prioritized dataset, which mainly
 203 uses UNFCCC (BUR and NC) data, unless such data are missing, in that case PRIMAP-hist uses
 204 extrapolated data from EDGAR (2021), FAO (2021) and BP Statistical Review of World Energy (2021).

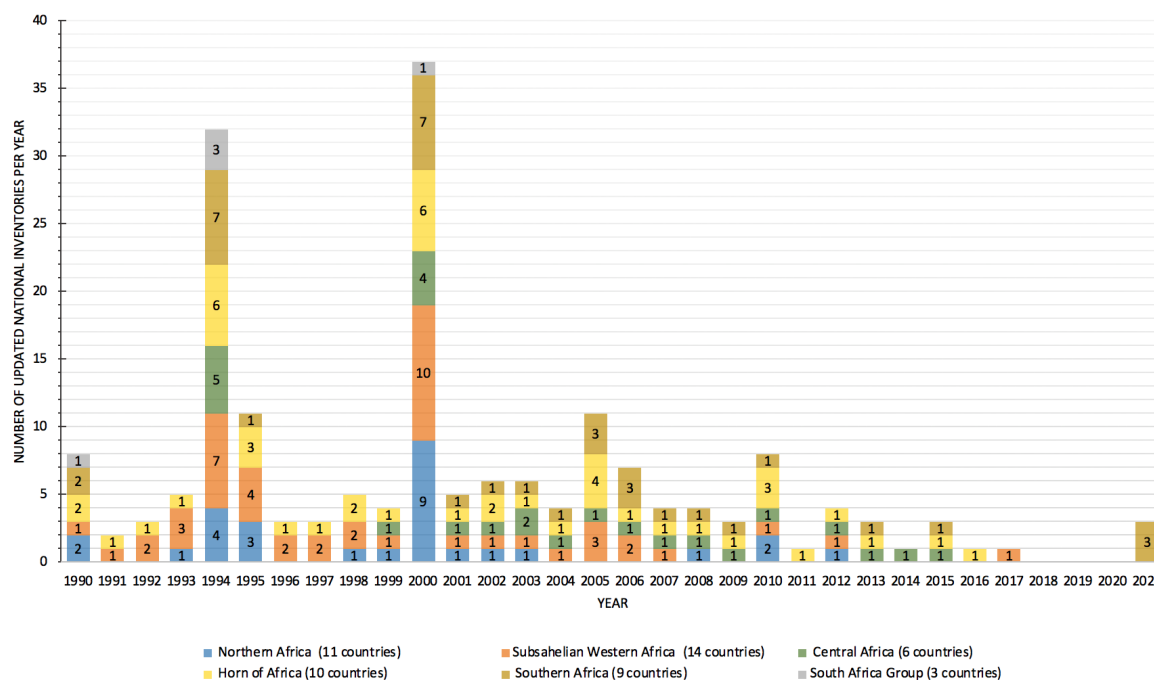


205 **Global Carbon Project (GCP) fossil CO₂ emissions**

206 We used country-level FCO₂ data published by the global CO₂ budget by the Global Carbon Project (GCP)
207 (Friedlingstein et al., 2020) separated per fuel type (gas, oil and coal) and including fossil fuel use in the
208 combined industry, ground transportation and power sectors, natural gas flaring, cement production, and
209 process-related emissions (e.g. fertilizers and chemicals). Data for African countries coming among others
210 from the Carbon Dioxide Information Analysis Center (CDIAC) compiled until 2018 (Gilfillan &
211 Marland, 2021), BP Statistical Review of World Energy (BP, 2020), and recent estimates of cement
212 production and clinker-to-cement ratios (Andrew, 2020).

213 **UNFCCC inventories for CO₂ in the LULUCF sector**

214 We used UNFCCC submissions for LULUCF CO₂ fluxes from NC and BUR reports downloaded from
215 the UNFCCC website (<https://unfccc.int/>) in March 2021, and further processed into .csv tables by Deng
216 et al., (2021). Those estimates are based on different accounting methods following the IPCC Guidelines
217 (IPCC, 2006; IPCC, 2019). African countries, being Non-Annex I countries, do not report emissions every
218 year. Figure 1 shows the number of BUR and NC provided each year per African region. The years 1990,
219 1994, 1995, 2000 and 2005 are featured with several updates, while most of the other years have few
220 updates. About every two years, all regions have at least one update. Note that flexibility for BUR is given
221 to Least Developed Countries (LDCs), that include 33 out of 56 African countries, and to Small Islands
222 Developing States (SIDS), that include six African countries (Table S3).



223 **Figure 1. Number of UNFCCC reports for LULUCF CO₂ fluxes in National Communications and Biennial**
 224 **Update Reports, per group of countries defined in Table S1.**

225 Non-Annex I African countries can use older versions of the IPCC guidelines (IPCC, 2006; IPCC, 2019a).
 226 This induces uncertainties from changes in accounting methods between versions, with recent guidelines
 227 having more detailed sectors and sources. There is no data for Libya, Equatorial Guinea, Malawi and Sierra
 228 Leone during the whole period. UNFCCC data are missing in some years for Rwanda, Sao Tome & Principe,
 229 Senegal, South Sudan, Angola. There is no data during 1990-1998 for Liberia.

230 We noticed that NC and BUR lack details regarding the methods used, the sources for activity data and
 231 emissions factors, and most of them are in French language. BUR in .pdf format include a non-standardized
 232 table for emissions. The reader is sometimes referred to the “national coordinator for climate change
 233 service” with no link to any database or contact person.

234 Because the PA targets human-induced emissions, countries use the proxy of “Managed lands” for the
 235 LULUCF sector, as defined by the IPCC guidelines ([https://www.ipcc-](https://www.ipcc-nggip.iges.or.jp/public/2006gl/vol4.html)
 236 [nggip.iges.or.jp/public/2006gl/vol4.html](https://www.ipcc-nggip.iges.or.jp/public/2006gl/vol4.html); last accessed in August 2022). Managed lands are areas where
 237 LULUCF CO₂ fluxes are assigned to some anthropogenic activities. Several African NC and BUR do not
 238 contain information on their managed lands areas. We thus looked at REDD+ national reports
 239 (<https://redd.unfccc.int/submissions.html?topic=6>; last accessed in August 2022) to get this information
 240 (Fig. S2 and Table S8). LULUCF CO₂ fluxes on managed lands result from either direct anthropogenic



241 effect such as land use change and forestry, or indirect effects (such as change in CO₂ and climate) on land
242 remaining in the same land use, e.g. forest remaining forest (Grassi et al., 2022). The vast majority of African
243 countries use a Tier 1 IPCC accounting method which does not distinguish between these different effects.
244 Tier 1 methods use a classification with only three out of six possible types of land: “forest land”, “cropland”
245 and “grassland”, and do not give spatially explicit land use data. Tier 2 methods include fluxes from six
246 land use types: forest, cropland and grassland, wetlands, urban and other land-use, for the case of land
247 remaining under the same land use type, and for the case of conversions between land use types. In Africa,
248 only South Africa and Zambia used Tier 2 methods for some LULUCF CO₂ subsectors.

249 **Processing of the UNFCCC LULUCF CO₂ data and outliers correction**

250 We processed the UNFCCC LULUCF CO₂ data for outlier corrections (Table S4). For Guinea-Bissau, and
251 Tanzania, we identified inconsistent values from successive communications with substantially differing
252 numbers. For Guinea, Madagascar, Zimbabwe, Congo, Mali, the Central African Republic (CAF), Angola
253 and Mauritius we identified changes of more than one order of magnitude between two consecutive reports
254 and likely implausibly large carbon sinks considering their national forest area. The computations of per
255 area emissions and removals showed discrepancies, which points out the need for further examination and
256 inspection of more recent reports in NDC and REDD+ reports (Table S4). Our corrections explained in the
257 supplementary section are consistent with those proposed by Grassi et al. (2022) who diagnosed
258 ‘biophysically impossible’ sequestration rates with a threshold value larger than 10 tCO₂/ha yr⁻¹ over an
259 area greater than 1 Mha. For Namibia, Nigeria and the Democratic Republic of the Congo (DRC), it was
260 challenging to select a best estimate between recent and past reports. For those countries, corrections using
261 more recent data than BUR /NCs have high uncertainties, as noted by Grassi et al. (2022). This includes the
262 absence of any sink for DRC for instance, contrary to sinks consistently reported over time and large forested
263 area in this country’s previous reports to the UNFCCC. We therefore systematically looked at corrected
264 values for both case scenarios (with and without Namibia, Nigeria and DRC data corrections). In total, we
265 corrected 13 outliers as shown in Table S4, consistently with Grassi et al. (2022).

266 **Food and Agriculture Organization of the United Nations (FAO) LULUCF CO₂ fluxes**

267 We used data from LULUCF CO₂ fluxes over 1990-2019 from the FAO Global Forests Resource
268 Assessments (FAO FRA; data License: CC BY-NC-SA 3.0 IGO, extracted from: <https://fra-data.fao.org>;
269 date of Access: May 2022). According to the 2005 FAO categories and definitions, forest is land covering
270 at least 0.5 hectares and having vegetation taller than 5 meters with a canopy cover higher than 10%. Other
271 wooded lands refer to land that are not classified as “forest” but that are wider than 0.5 ha, have a canopy
272 cover of 5%-10% or combine trees, shrubs and bushes with cover higher than 10%. The FAO data for forests



273 comprise carbon stock changes from both aboveground and belowground living biomass pools. They are
274 independent from country-reported UNFCCC emissions and removals. The FAO estimates are based on
275 activity data, areas of forest land and CO₂ emissions and removals factors. The FAO data reports: 1) net
276 emissions and removals from “forest land remaining forest land” and from “land converted to forest”
277 grouped together, and 2) emissions from “net forest conversion”, i.e. deforestation. In contrast, the UNFCCC
278 accounting uses a 20-years window for CO₂ fluxes from land use change, while land-use change fluxes from
279 land-converted-to-forest are reported separately from those of ‘forest remaining forest’.

280 **1.3 Dynamic Global Vegetation Models (DGVM)**

281 We used Net Biome Productivity (NBP) from 14 Dynamic Global Vegetation Models (DGVM) from the
282 TRENDY v9 ensemble covering the period 1990-2019. The different models described in Friedlingstein et
283 al. (2019) are: CABLE, CLASS, CLM5, DLEM, ISAM, JSBACH, JULES, LPJ, LPX, OCN, ORCHIDEE-
284 CNP, ORCHIDEE-SDGVM, and SURFEX (Table S5). DGVM are forced by historical reconstructions of
285 land cover change, atmospheric CO₂ concentration and climate since 1901. Detailed cropland management
286 practices are generally ignored, except for the harvest of crop biomass. Forest harvest is prescribed from
287 historical statistics in 11 models (Table A1, of Friedlingstein et al., (2020)). The models simulate carbon
288 stock changes in biomass, litter and soil pools. From the difference between simulations with and without
289 historical land cover change, a flux called ‘land use emissions’ can be obtained from DGVM. This flux
290 includes the indirect effects of climate and CO₂ on lands affected by land use change, and a foregone sink
291 called “loss or gain of atmospheric sink capacity”, which is absent from the methods used by UNFCCC and
292 FAO. Thus, land use change fluxes from DGVM were not compared with other estimates. Note that DGVM
293 do not explicitly separate managed and unmanaged land. Thus, we used all forest lands to calculate their
294 mean CO₂ fluxes.

295 **1.4 Atmospheric inversions**

296 **CO₂ inversions**

297 We used the net land CO₂ fluxes excluding fossil fuel emissions (hereafter, net ecosystem exchange) from
298 three global inversions of the Global Carbon Project that cover a long period (see Table A4 of Friedlingstein
299 et al., 2020), including : CarbonTrackerEurope (CTRACKER-EU-v2019; van der Laan-Luijkx et al., 2017),
300 the Copernicus Atmosphere Monitoring Service (CAMSV18-2-2019; Chevallier et al., 2005), and one
301 variant of Jena CarboScope (JENA, sEXTocNEET_v2020; Rödenbeck et al., 2005). The GCP inversion
302 protocol recommends to use as a fixed prior the same gridded dataset of FCO₂ emissions (GCP-GridFED).
303 However, some modelers used different interpolations of this dataset, and one group used a different gridded



304 dataset (Ciais et al., 2021). We applied a correction to the estimated total CO₂ flux by subtracting a common
305 FCO₂ flux from each inversion (Figure S8 and Methodological Supplementary 2). The resulting land
306 atmosphere CO₂ fluxes, or net ecosystem exchange, cannot be directly compared with inventories aiming
307 to assess C stock changes, given the existence of land-atmosphere CO₂ fluxes caused by lateral processes.
308 This issue was discussed by Ciais et al. (2021) and a practical correction of inversions was proposed by
309 Deng et al. (2022) based on new datasets for CO₂ fluxes induced by lateral processes involving river
310 transport, crop and wood product trade. We applied here the same correction to all CO₂ inversions.

311 **CH₄ inversions**

312 We used the CH₄ emissions from global inversions over 2000-2017 from the Global Methane Budget
313 (Saunois et al., 2020) (Table 1). This ensemble includes 11 models using GOSAT satellite CH₄ total-column
314 observations covering 2010-2017, and 11 models assimilating surface stations data (SURF) since 2000
315 (Table S4). Surface inversions are constrained by very few stations for Africa, while the GOSAT satellite
316 data has a better coverage. One could thus expect GOSAT inversions to give more robust results. Inversions
317 deliver an estimate of surface net CH₄ emissions, although some of them solve for fluxes in groups of
318 sectors, called ‘super-sectors’. In the inversion dataset, net CH₄ surface emissions were interpolated into a
319 0.8° × 0.8° resolution, regridded from coarser resolution fluxes and separated into ‘super-sectors’ either
320 using prior emission maps or posterior estimates for those inversions solving fluxes per supersector,
321 following Saunois et al., (2020). More specifically, these five super-sectors are: 1) Fossil Fuel, 2)
322 Agriculture and Waste, 3) Wetlands, 4) Biomass and Biofuel Burning (BBUR), and 5) Other natural
323 emissions. We separated CH₄ anthropogenic emissions from inversions using Method 1 and Method 2
324 proposed by Deng et al. (2021). Method 1 relies on the separation calculated by each inversion except for
325 the BBUR supersector from which wildfire emissions were subtracted based on the Global Fires Emission
326 Dataset (GFED) version 4 (van der Werf et al., 2017). Method 2 removes from total emissions the median
327 of natural emissions from inversions (Deng et al. 2022). The two methods gave similar results and only
328 Method 1 was used in the results section.

329 **N₂O inversions**

330 We used three N₂O atmospheric inversions from the global N₂O budget synthesis (Tian, 2020) and from
331 Deng et al. (2022) (Tables S1, S7) : PyVAR CAMS (Thomson et al., 2014), MATCM_JMASTEC
332 (Rodgers, 2000), (Patra et al., 2018), and TOMCAT (Wilson et al., 2014; Monks et al., 2017). We use the
333 total N₂O flux from inversions including natural emissions, given that natural emissions estimates are highly
334 uncertain for Africa. Inversion results are therefore not directly comparable with the PRIMAP-hist inventory
335 which only contains anthropogenic emissions.



336 **1.5 Metrics to compare gasses and ancillary data**

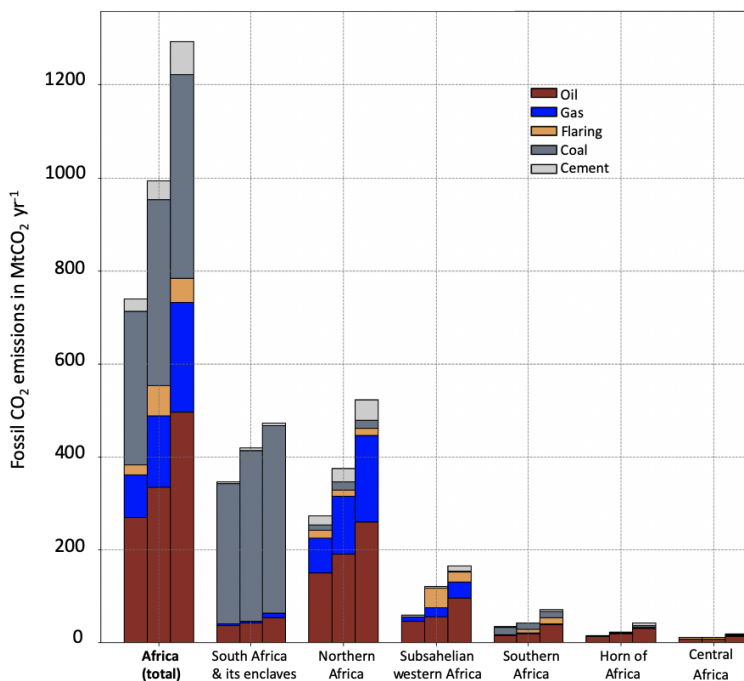
337 We express emissions of non-CO₂ gasses in megatons of carbon dioxide equivalent (MtCO₂e) using the
338 Global Warming Potential over a 100-year time horizon (GWP100) values from the fourth IPCC
339 Assessment Reports (IPCC AR4, WGI Chapter 2, 2007), consistent with PRIMAP-hist and country-reported
340 data. We used population data from the United Nations population (World Population Prospects 2019:
341 Highlights | Multimedia Library - United Nations Department of Economic and Social Affairs, 2022), for
342 computing per capita FCO₂ emissions and their disparities, based on Gini indices (Dortman et al.,1979) for
343 measuring statistical dispersions among a given population (methodological supplementary M1). We also
344 used African GDP data (World Bank, 2017).

345 **2 Results and discussion**

346 **2.1 Fossil CO₂ emissions**

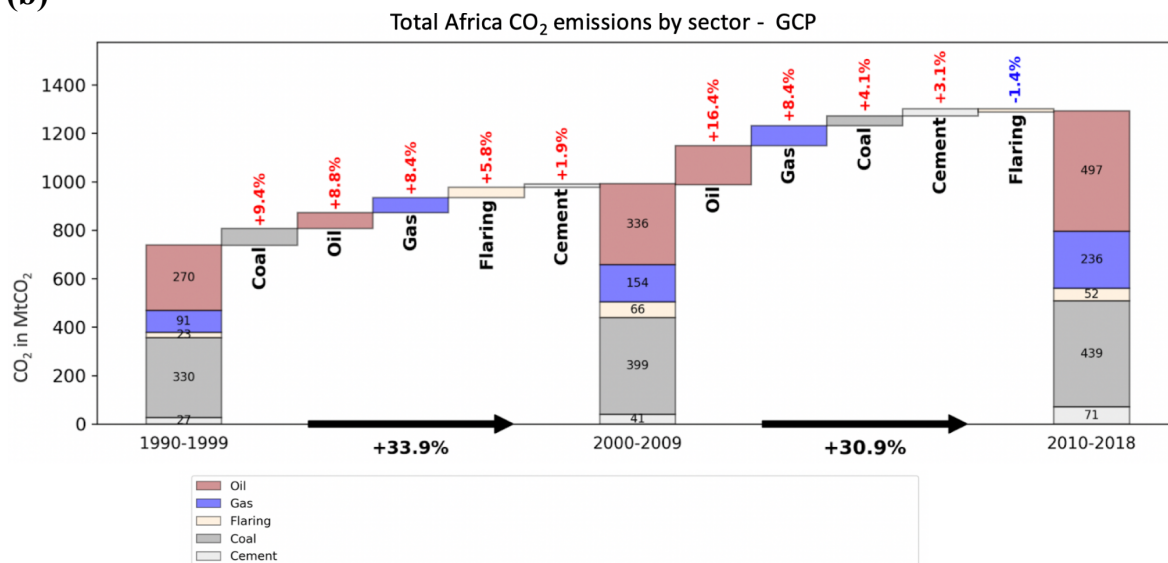
347 **2.1.1 Continental, regional and country changes**

(a)

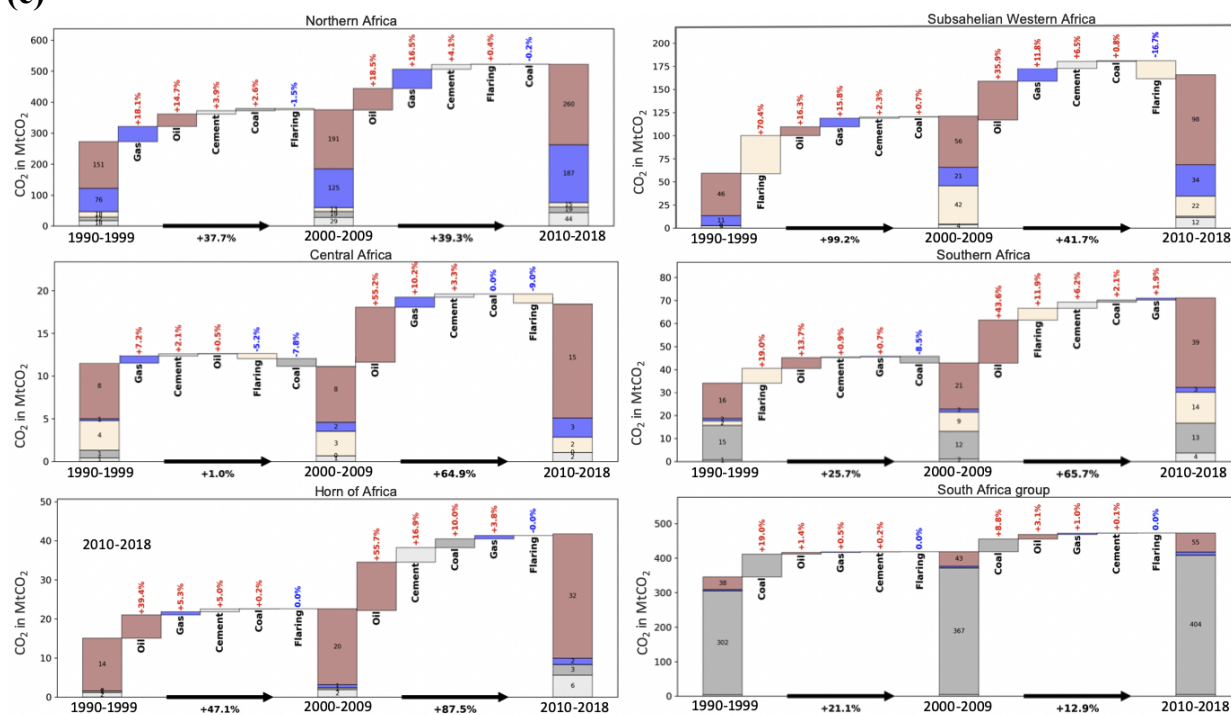




(b)

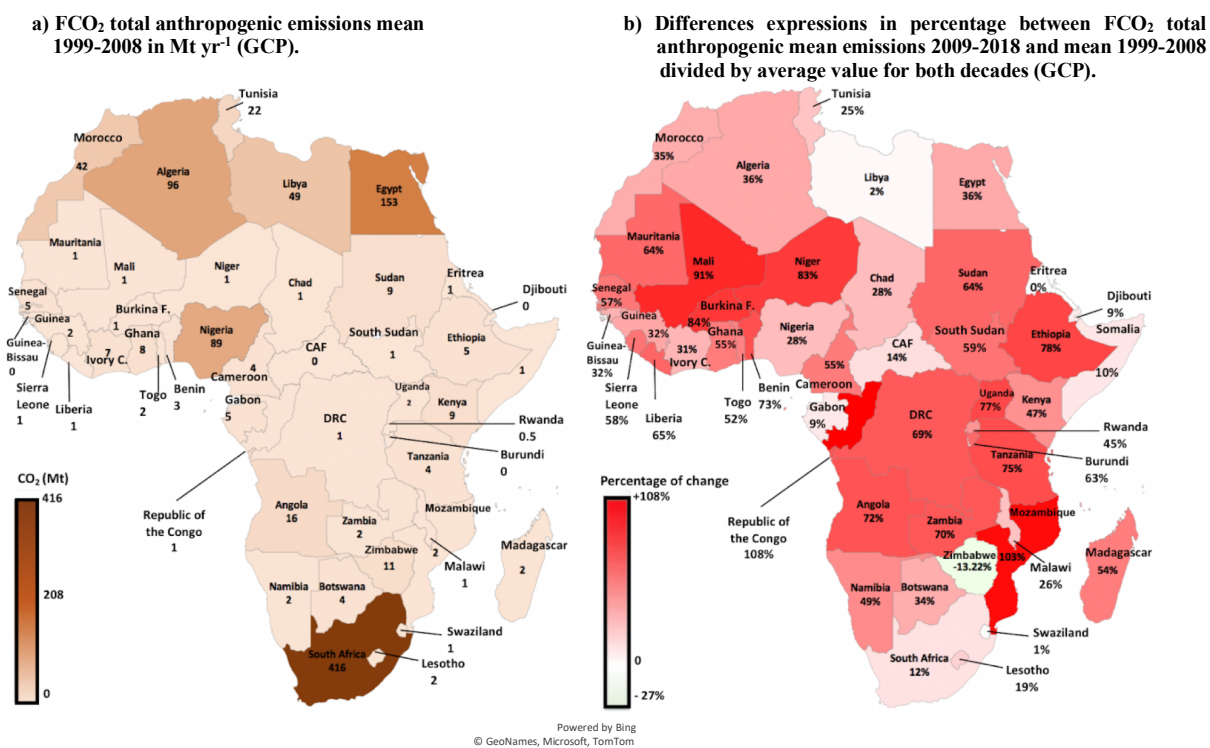


(c)



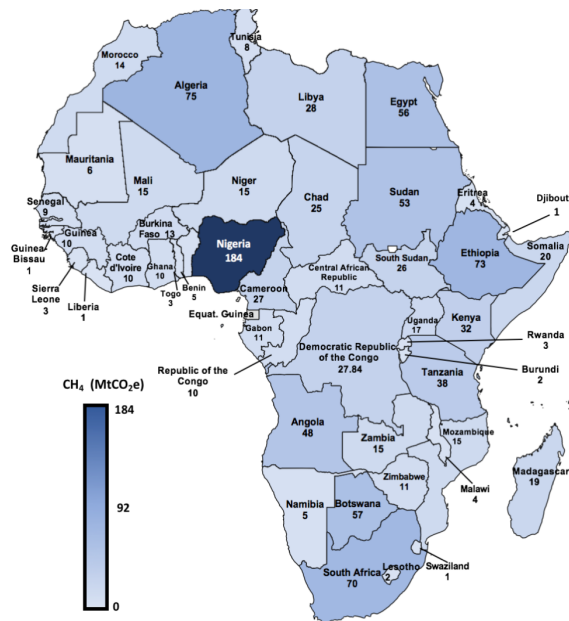


348 Figure 2. (a) African fossil fuel CO₂ emissions per fuel type and for cement per region over 1990-1999, 2000-2009
 349 and 2010-2018. (b) Contribution of each fuel type to the change of African emissions. (c) Same for different regions
 350 regrouping several countries. Data from GCP (2019).

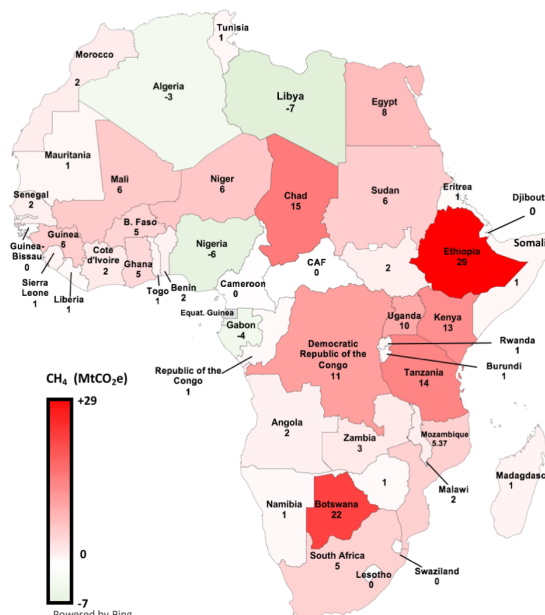




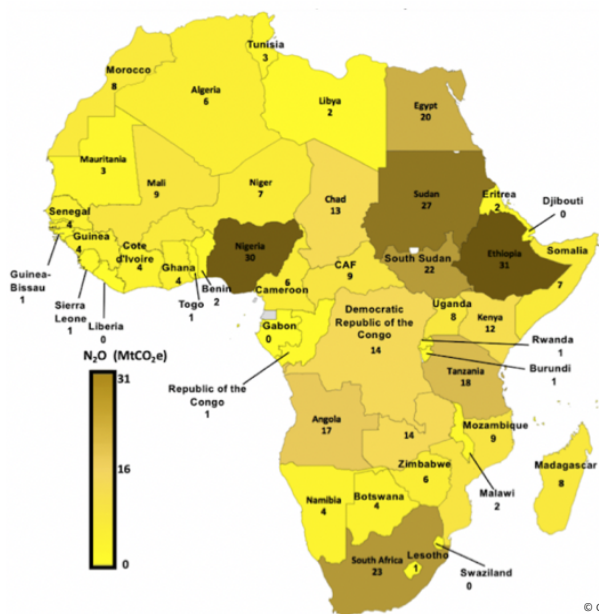
c) CH₄ total anthropogenic emissions mean 1999-2008 in MtCO₂e yr⁻¹ (PRIMAP-hist).



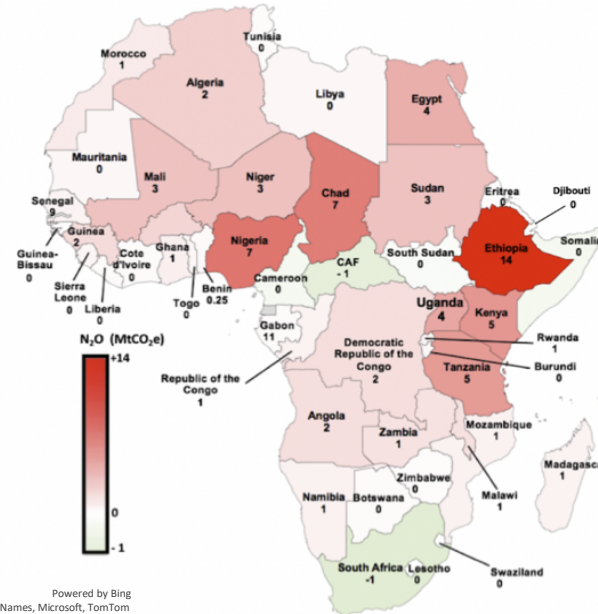
d) Differences between CH₄ total anthropogenic mean emissions 2009-2018 and mean 1999-2008 in MtCO₂e yr⁻¹ (PRIMAP-hist).



e) N₂O total anthropogenic emissions mean 1999-2008 in MtCO₂e yr⁻¹ (PRIMAP-hist).



f) Differences between N₂O total anthropogenic mean emissions 2009-2018 and mean 1999-2008 in MtCO₂e yr⁻¹ (PRIMAP-hist).





351 **Figure 3 (a). Maps of average fossil fuel CO₂ emissions for African countries during 1999-2008 in MtCO_{2e} yr⁻¹ and**
352 **(b) change from 1999-2008 to 2009-2018 using data from GCP in MtCO_{2e} yr⁻¹ (Friedlingstein et al., 2019); (c-d)**
353 **same but with anthropogenic CH₄ emissions from PRIMAP-hist in MtCO_{2e} yr⁻¹; (e-f) same for anthropogenic N₂O**
354 **emissions from PRIMAP-hist in MtCO_{2e} yr⁻¹.**

355 PRIMAP-hist and GCP

356 First, we compared GCP and PRIMAP-hist fossil CO₂ emissions. We found that most of the relative differences
357 between these two datasets at country level considerably decreased with time, except for Mali. Those
358 differences are less than 5% for most of the main African emitters during the last decade, except for South
359 Africa where the difference is a bit larger than 10% (see maps in Fig. S7). The largest relative difference
360 between the two datasets comes from Mali in the decade 2009-2018, with FCO₂ emissions of 3 MtCO₂ yr⁻¹ in
361 GCP, compared to 1 MtCO₂ yr⁻¹ in PRIMAP-hist. Given the relatively small differences, we chose to use only
362 GCP for trends between decades, but when computing net budgets for the three main GHG, we show
363 differences between the use of those two estimates.

364 The changes of African FCO₂ emissions per fuel type and for cement using the GCP data are shown in Fig. 2
365 (a). In Fig.2 (b), we show absolute values and relative contributions to the total change in each decade. During
366 2010-2018, total African FCO₂ emissions from oil (497 MtCO₂ yr⁻¹) and coal (439 MtCO₂ yr⁻¹) were roughly
367 similar. While global FCO₂ emissions increased by +13 % over this period (Friedlingstein et al., 2019), African
368 FCO₂ almost doubled in 2018 compared to 1990 levels, a relative increase comparable with that of China over
369 the same period. From 1990-1999 to 2000-2009, the mean emissions increased by 33.9% from 741 MtCO₂ yr⁻¹
370 to 996 MtCO₂ yr⁻¹. All FCO₂ sectors contributed to this decadal increase. The contribution from coal (+9.4
371 %) was slightly larger but comparable to that from oil (+9 %) and gas (+8 %). From 2000-2009 to 2010-2018,
372 emissions further increased by 31% from 996 MtCO₂ yr⁻¹ to 1295 MtCO₂ yr⁻¹. The oil and the gas fuels
373 contributed the most to this increase with +16 % for oil, and +8 % for gas. Coal emissions increased by only
374 +4.1 % and coal went from being the first source of African FCO₂ emissions over 2000-2009 to the second one
375 over 2010-2018.

376 As for regional contributions to emissions changes between 1990-1999 and 2000-2009 shown in Fig. 2 (b) the
377 main contribution to the total increase came from the region of South Africa where emissions increased from
378 302 MtCO₂ yr⁻¹ to 367 MtCO₂ yr⁻¹ (+21.1 %, coal being the largest contributor). The second largest contribution
379 to the increase is from North Africa where oil was the largest contributor (emissions increased from 151 MtCO₂
380 yr⁻¹ to 191 MtCO₂ yr⁻¹; +15 %), and gas (+18%). The least increasing region was Central Africa. North Africa
381 experienced the largest increase from 1990-1999 to 2000-2009, and from 2000-2009 to 2010-2018 with



382 successive increases of +38 % and +39 %, largely dominated by oil and gas (Fig. 4 (b)). As a result, during the
383 period 2010-2018, Northern African countries were the dominant emitters with 545 MtCO₂ yr⁻¹. The group of
384 South Africa (including Lesotho and Botswana) was the second biggest emitter region over 2010-2018, mainly
385 due to coal emissions from the Republic of South Africa. The two least contributing African regions were the
386 Horn of Africa and Central Africa.

387 At the country level, Figure 3a-b shows mean FCO₂ emissions and relative changes over the last two decades.
388 The main emitters do not have the biggest relative changes. The four main emitters over 2000-2009 were South
389 Africa (416 MtCO₂ yr⁻¹), Egypt (153 MtCO₂ yr⁻¹), Algeria (96 MtCO₂ yr⁻¹) and Nigeria (89 MtCO₂ yr⁻¹). Those
390 four countries altogether represented 67% of the continental total emissions over 2000-2009 (987 MtCO₂ yr⁻¹).
391 The largest relative increases from 2000-2009 to 2010-2018 are from Congo (+108 %), Mozambique (+103 %)
392 and Mali (91%), compared to relative increases in the main emitters, the Republic of South Africa (+21 %),
393 Egypt (+36%) and Algeria (+36%).

394 2.1.2 Variations of per capita and per GDP fossil fuel CO₂ emissions

395 Per capita emissions

396 Using ancillary data on population (Fig. S2 and Fig. S3) we computed the mean African per capita emissions
397 of 1 tCO₂/cap yr⁻¹ for 2009-2018 (Figures S2 and S3), which is 5 times larger than during 1990-1998 (0.2 tC/cap
398 yr⁻¹), and yet 5 times smaller than the global average (5 tCO₂/cap yr⁻¹). From 1999-2008 to 2009-2018, African
399 per capita emissions increased by 30 %. African per capita FCO₂ emissions during 2009-2018 were 17 times
400 less than in the USA (17 tCO₂/cap yr⁻¹), 7 times less than in China (7 tCO₂/cap yr⁻¹), 7 times less than in
401 EU27+UK (7 tCO₂/cap yr⁻¹), and 2 time less than India (2 tCO₂/cap yr⁻¹). At the country level, the biggest per
402 capita emissions over 2009-2018 were from the Republic of South Africa with 9 tCO₂/cap yr⁻¹, which ranks
403 14th worldwide, above China and just below Poland. The second biggest per capita emissions were from Libya
404 (8 tCO₂/cap yr⁻¹). The smallest ones were from the DRC (0.1 tCO₂/cap yr⁻¹). For the first period 1990-1998,
405 per capita emissions of African region ranked in this order: South Africa group (4 tCO₂/cap yr⁻¹) > Northern
406 Africa (2 tCO₂/cap yr⁻¹) > Central African countries (1 tCO₂/cap yr⁻¹) > Southern countries (0.8 tCO₂/cap yr⁻¹)
407 > Horn of Africa (0.5 tCO₂/cap yr⁻¹) > Sub-Saharan Western Africa (0.3 tCO₂/cap yr⁻¹). For the second period
408 2009-2018, they ranked in this order: South Africa group (4 tCO₂/cap yr⁻¹) > Northern Africa (2 tCO₂/cap yr⁻¹)
409 > Southern countries (1 tCO₂/cap yr⁻¹) and Horn of Africa (1 tCO₂/cap yr⁻¹) > Central Africa countries (1
410 tCO₂/cap yr⁻¹) > Sub-Saharan Western Africa (0.4 tCO₂/cap yr⁻¹). At country scale during the first period of
411 1990-1998, the four African largest per capita emissions ranked in this order: Libya (9 tCO₂/cap yr⁻¹) > the
412 Republic of South Africa (9 tCO₂/cap yr⁻¹) > Gabon (5 tCO₂/cap yr⁻¹) > Algeria (3 tCO₂/cap yr⁻¹). The four



413 African countries with the smallest per capita emissions ranked as following: Burundi ($0.04 \text{ tCO}_2/\text{cap yr}^{-1}$) <
414 Uganda, Ethiopia and Mali ($0.1 \text{ tCO}_2/\text{cap yr}^{-1}$).

415 We also computed the GINI index for African per capita FCO₂ emissions for each of the last three decades,
416 using data from (Friedlingstein et al., 2020) (see Methodological Supplementary M2). These GINI values were
417 0.7 for 1990-1998, 0.7 for 1999-2008, and 0.7 for 2009-2018, thus very stable over the last 30 years and close
418 to 1, indicating high inequities among countries.

419 **Emissions per GDP**

420 **Per exchange rate vs. per Purchasing Power Parities (PPP) GDP**

421 According to the International Monetary Fund (IMF), the Gross Domestic Product (GDP) delivers an estimate
422 “of the monetary value of goods and services produced in a country over a chosen period.” GDP data from the
423 World Bank (2015) is available for 30 African countries only (Fig. S4). The four countries with the biggest per
424 \$US exchange rate GDP (Fig. S5) are: Nigeria (\$490 B) > South Africa (\$350B) > Egypt (\$330B) and Algeria
425 (\$330B) > Angola (\$120B). The four countries with the smallest GDP in 2015 are: Gambia (\$1.4B) and
426 Seychelles (\$1.4B) > Guinea-Bissau (\$1B) > Comoros (\$970 M). Emissions per \$US GDP are shown in Fig.
427 S5 The Purchasing Power Parities (PPP) calculated by the International Comparison Program (ICP) of the
428 World Bank is a refined measure of what a given national currency can acquire in terms of goods or services
429 in another country, removing the impact of currency exchange rates. Emissions per PPP\$ GDP are shown in
430 Fig. S6.

431 The mean of African emissions per unit PPP\$ GDP in 2016 was $0.6 \text{ kgCO}_2/\text{PPP\$ yr}^{-1}$, which is more than twice
432 the global value, 3 times the mean value of the USA ($0.2 \text{ kgCO}_2/\text{PPP\$ yr}^{-1}$) and Europe ($0.2 \text{ kgCO}_2/\text{PPP\$ yr}^{-1}$).
433 This points to a more carbon intensive economic growth in Africa than in developed countries, which may
434 be an important barrier for future mitigation strategies as the GDP of Africa has grown by 112% in the last 30
435 years, and is projected to increase in the future by 3% per year (World Bank, 2022). At regional level, the
436 largest values were: South Africa ($0.4 \text{ kgCO}_2/\text{PPP\$ yr}^{-1}$) > North Africa, Southern Countries and Sahelian
437 Western Africa ($0.2 \text{ kgCO}_2/\text{PPP\$ yr}^{-1}$) > Central Africa and the Horn of Africa ($0.1 \text{ kgCO}_2/\text{PPP\$ of GDP}$). At
438 country scale, the largest emitters per unit of GDP were Libya ($0.7 \text{ kgCO}_2/\text{PPP\$ yr}^{-1}$) and South Africa (0.7
439 $\text{kgCO}_2/\text{PPP\$ yr}^{-1}$) > Lesotho ($0.4 \text{ kgCO}_2/\text{PPP\$ yr}^{-1}$) > Algeria ($0.3 \text{ kgCO}_2/\text{PPP\$ yr}^{-1}$) (Fig. S6.) The smallest
440 emitters were: DRC ($0.03 \text{ kgCO}_2/\text{PPP\$ yr}^{-1}$) < Chad ($0.04 \text{ kgCO}_2/\text{PPP\$ yr}^{-1}$) < Burundi ($0.06 \text{ kgCO}_2/\text{PPP\$ yr}^{-1}$)
441 < Uganda ($0.07 \text{ kgCO}_2/\text{PPP\$ yr}^{-1}$).

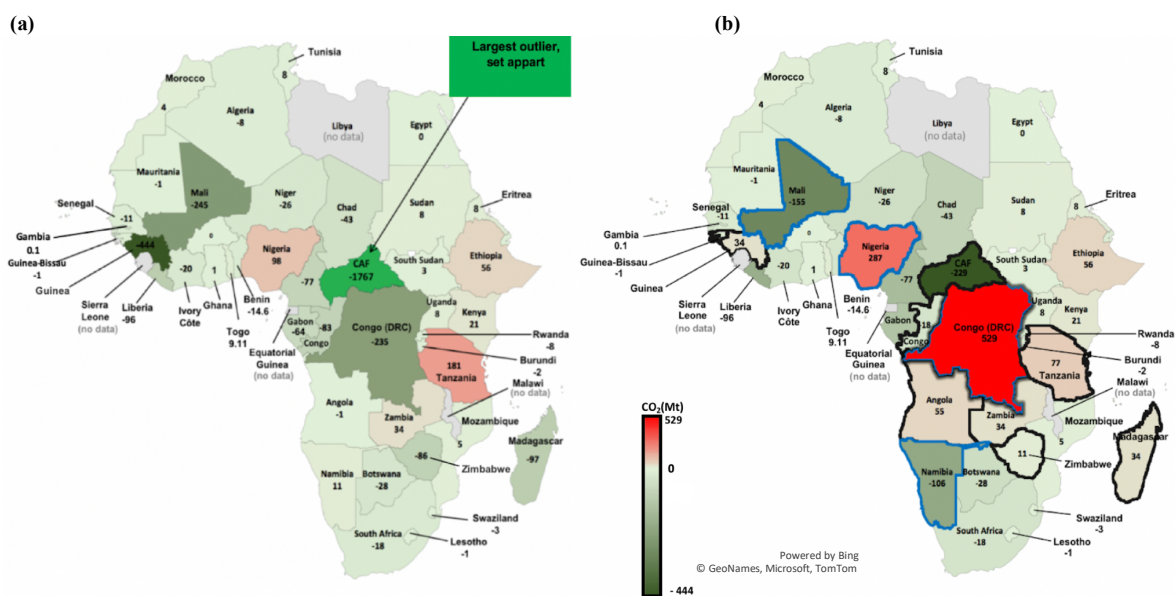
442 We also used GDP per unit exchange rate from the International Energy Agency (IEA, 2019). The mean African
443 emissions per unit of $\text{GDP}_{\text{exch.rate}}$ was $0.5 \text{ kgCO}_2 \text{ \$/\$ yr}^{-1}$, larger than elsewhere, except in Asia (0.6
444 $\text{kgCO}_2/\text{GDP}_{\text{exch.rate}} \text{ yr}^{-1}$). As shown in Fig. S5, over 2013-2017 the six biggest emitters were South Africa (0.7

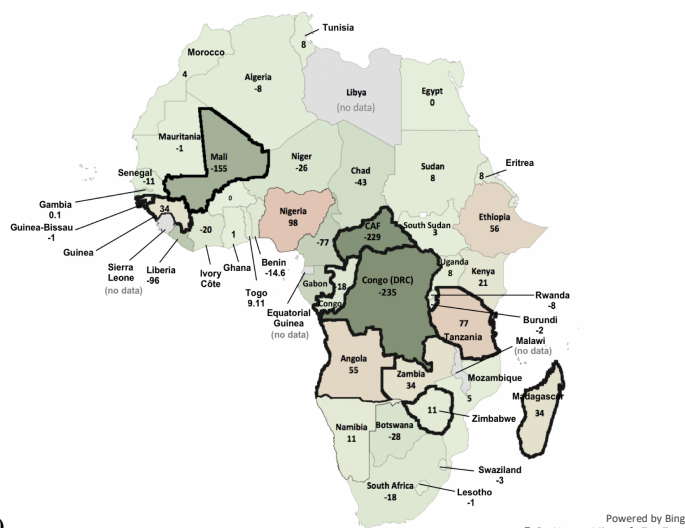


445 $\text{kgCO}_2/\text{GDP}_{\text{exch.rate}} \text{ yr}^{-1}$) > Libya (0.5 $\text{kgCO}_2/\text{GDP}_{\text{exch.rate}} \text{ yr}^{-1}$) > South Sudan (0.4 $\text{kgCO}_2/\text{GDP}_{\text{exch.rate}} \text{ yr}^{-1}$)
 446 > Zimbabwe, Benin and Algeria (0.3 $\text{kgCO}_2/\text{GDP}_{\text{exch.rate}} \text{ yr}^{-1}$). The correlation coefficient between
 447 $\text{GDP}_{\text{exch.rate}}$ and FCO_2 emissions per $\text{GDP}_{\text{exch.rate}}$ was 0.3, suggesting that the countries with a high GDP do
 448 not always emit more CO_2 per unit GDP. For instance, South Africa ranked first with 0.7 $\text{kgCO}_2/\text{GDP}_{\text{exch.rate}}$
 449 yr^{-1} and second for GDP (350 \$Billion); Nigeria ranked first for GDP (490 \$Billion), but 21st for emissions per
 450 GDP (0.1 $\text{kgCO}_2/\text{GDP}_{\text{exch.rate}} \text{ yr}^{-1}$). This may be related to the fact that countries with a high GDP are also
 451 more likely to create growth through sustainable activities.

2.2 LULUCF CO_2 fluxes

Outlier corrections





454 **Figure 4. Map of national LULUCF CO₂ fluxes for 2001-2018 in MtCO₂ yr⁻¹. (a) before outliers' removals.**
455 **((b) After outliers' removal according to Grassi et al. (2022). (c) After outlier removals (DRC, Namibia and**
456 **Nigeria) from this study. Positive values represent a net C loss by ecosystems.**

457 In this section, we analyze CO₂ fluxes from the LULUCF sector, based on UNFCCC data (section 1.1)
458 which include forest lands, grasslands, croplands, and all possible conversions between them (IPCC,
459 2003; 2006). As shown in section 1.2 and Table S4, we found that some countries' reports are outliers
460 with biophysically implausible CO₂ sinks and/or sudden unexplained very large changes between
461 successive reports. Due to scarce data over 1990-1998 we focus on the period 2001-2018. In the
462 following paragraph, we discuss four approaches to include UNFCCC data:

463 a) Uncorrected data, b) corrections following Grassi et al. (2022) for all countries, c) corrections
464 following Grassi et al. (2022) except DRC, Namibia and Nigeria, d) Corrections following Grassi et al.
465 (2022) except DRC.

466 Figure 4 (a) shows UNFCCC data without correcting for outliers, based on BUR and NC data accessed
467 in May 2022. The majority of countries are sinks, or small sources, except Tanzania and Nigeria being
468 large sources. Very large (implausible) sinks are seen in Guinea and CAF. The continent is a CO₂ sink
469 of -3309 MtCO₂ yr⁻¹ during the period 2001-2018.

470 Figure 4 (b) shows the corrected fluxes according to Grassi et al. (2022) who excluded implausible large
471 sink rates and used NDC and REDD+ reports instead of NC data for DRC, Congo, CAF, Guinea,
472 Madagascar and the most recent BUR, NC and inventory data for Namibia, Angola, Zimbabwe and
473 Nigeria (see their Table 7). Africa as a whole is a CO₂ source of 265 MtCO₂ yr⁻¹. At regional scale, the
474 mean CO₂ sources distributes as follows on four regions: Sub-Saharan West Africa (235 MtCO₂ yr⁻¹) >
475 Horn of Africa (153 MtCO₂ yr⁻¹) > Central Africa (144 MtCO₂ yr⁻¹) > Southern Africa (14 MtCO₂ yr⁻¹).



476 The two sink regions are North Africa ($-259 \text{ MtCO}_2 \text{ yr}^{-1}$) and South Africa ($-23 \text{ MtCO}_2 \text{ yr}^{-1}$). At country
477 scale, after the corrections of Grassi et al. (2022), the four countries with the larger sinks are: CAF (-229
478 $\text{MtCO}_2 \text{ yr}^{-1}$) > Mali ($-155 \text{ MtCO}_2 \text{ yr}^{-1}$) > Namibia ($-106 \text{ MtCO}_2 \text{ yr}^{-1}$) > Cameroon ($-77 \text{ MtCO}_2 \text{ yr}^{-1}$). The
479 four countries with largest sources are DRC ($529 \text{ MtCO}_2 \text{ yr}^{-1}$) > Nigeria ($287 \text{ MtCO}_2 \text{ yr}^{-1}$) > Tanzania
480 ($77 \text{ MtCO}_2 \text{ yr}^{-1}$) > Ethiopia ($56 \text{ MtCO}_2 \text{ yr}^{-1}$). A main issue with the correction from Grassi is that it reports
481 no sink in DRC which has an important forest coverage representing 68% of the country area (FAO,
482 2015) and for which a sink was consistently reported in previous NCs.

483 Figure 4 (c) shows LULUCF CO_2 in African countries that are consistent with Grassi et al. (2022) except
484 for three countries: Namibia (we used 2000 NC3 instead of NIR2019), Nigeria (we used 2014 NC2
485 instead of 2017 BUR2) and DRC (we used 2015 NC3 instead of 2021 NDC). In that approach Africa
486 becomes a net CO_2 sink of -589 Mt yr^{-1} over 2001-2018. At regional scale, the region of Central Africa
487 (-620 MtCO_2) remains the main sink. But the values and ranking of the top sources rank as: Horn of
488 Africa (153 MtCO_2) > Southern Africa (141 MtCO_2) > Sub-Saharan West Africa (19 MtCO_2). At country
489 scale with this correction choice, the top sinks are: DRC (-235 MtCO_2) > CAF (-229 MtCO_2) > Mali ($-$
490 155 MtCO_2); and the three top sources: Nigeria (98 MtCO_2) > Tanzania (77 MtCO_2) > Ethiopia (56
491 MtCO_2).

492 In the fourth approach where we use the corrections of Grassi et al. (2022) except for DRC where we
493 kept the latest national communication instead of the most recent NDC, the continent is a net sink of $-$
494 $504 \text{ MtCO}_2 \text{ yr}^{-1}$ over 2001-2018. At regional scale, Central Africa is a large CO_2 sink, and the ranking
495 of sink regions is: Central African group ($-620 \text{ MtCO}_2 \text{ yr}^{-1}$) > North Africa ($-259 \text{ MtCO}_2 \text{ yr}^{-1}$) > South
496 Africa ($-23 \text{ MtCO}_2 \text{ yr}^{-1}$). The ranking of the source regions stays unchanged. At the country scale, the
497 main sink is DRC ($-235 \text{ MtCO}_2 \text{ yr}^{-1}$). In the paper, we will mainly use data corrected following Grassi et
498 al. (2022), but we want to raise a caution flag that adopting their correction for DRC had an enormous
499 effect on the CO_2 budget of the continent, which becomes a source. Using the original latest national
500 communication of DRC instead of the NDC used by Grassi et al., and our own corrections for Namibia
501 and Nigeria instead of those of Grassi et al. increased the continental CO_2 uptake.

502 **Comparison of UNFCCC managed land area and FAO forest and other wooded lands areas**

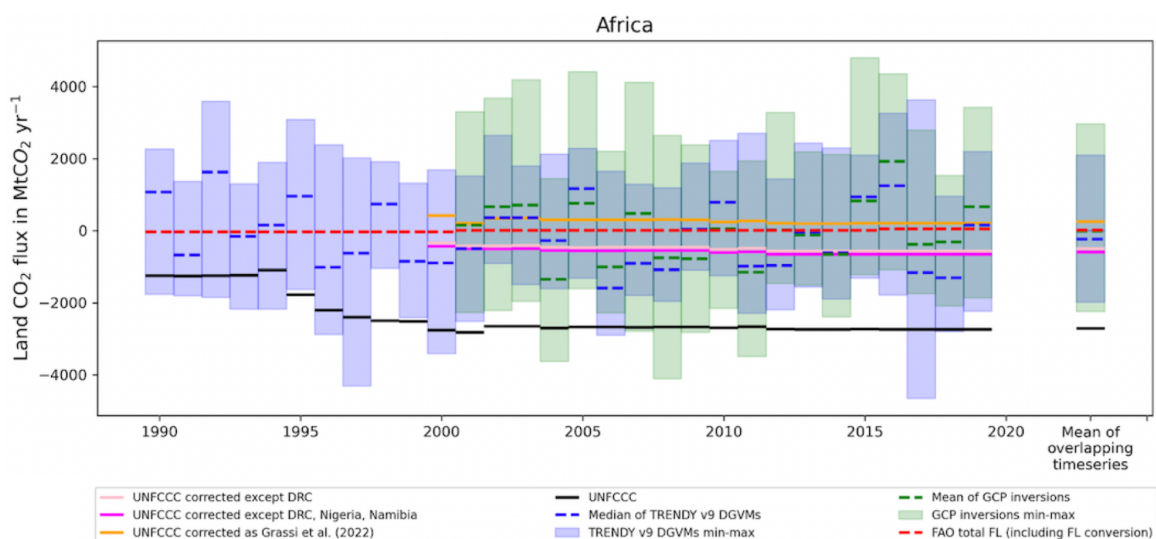
503 Figure S10 shows a comparison of land areas reported in NC, BUR and REDD+ reports
504 (<https://redd.unfccc.int/submissions.html?mode=browse-by-country>) with FAO forest land areas (2015)
505 and FAO forest land + other woodlands areas for the year 2015 (see Table S8). Consistent with Grassi
506 et al. (2022), all forest lands in Africa are considered as managed. We found that FAO forest lands areas
507 are closer to UNFCCC estimates than the sum of FAO forest and other woodlands area, except for DRC,

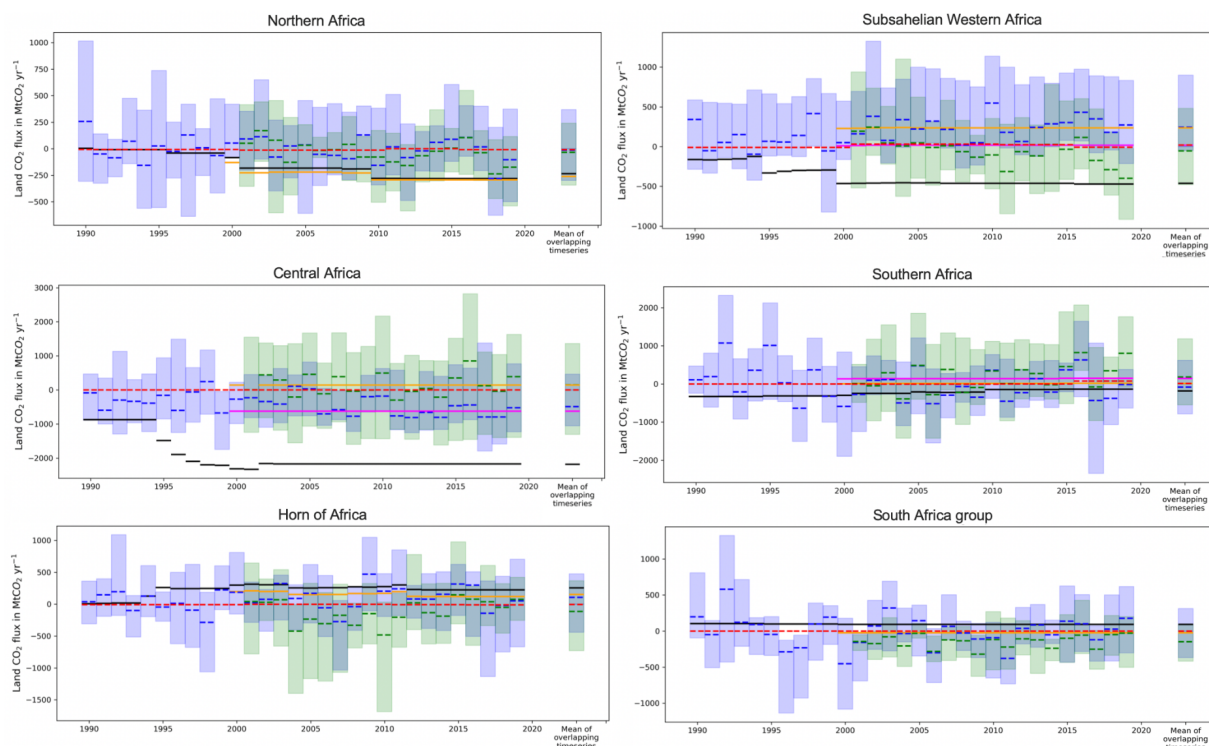


508 Sudan, Senegal, Niger and Mauritania (Table S8). Forest areas in UNFCCC data using IPCC default
509 method do not exactly match FAO data estimates of forest area.

510 LULUCF CO₂ fluxes from UNFCCC versus DGVM and inversions

511 A comparison between LULUCF CO₂ fluxes from UNFCCC, FAO, DGVMs and inversions is shown
512 in Fig. 5 at the scale of the continent and for the six regions. The period of overlapping time series is
513 2001-2018. For the continent, DGVMs give a mean sink of -232 MtCO₂ yr⁻¹ with a huge range from -
514 1977 MtCO₂ yr⁻¹ to 2095 MtCO₂ yr⁻¹. The years with the biggest sinks for DGVM (from the median of
515 all models) are 2006 and 2018, and the years with the smallest sinks are 2005 and 2016 which seem
516 related to widespread drought years across Africa. A key result shown by this figure is that the DGVMs
517 and inversions show a huge spread, making them of little value to ‘verify’ inventories for LULUCF
518 CO₂ fluxes in Africa. Yet, we observed that the median of all DGVM points to a sink for Africa, unlike
519 the UNFCCC data with the correction from Grassi et al. (2022).





520 **Figure 5. LULUCF CO₂ emissions and sinks: comparison between UNFCCC national greenhouse gas**
521 **inventories, TRENDYv9 DGVMs and inversions, for total Africa and for each of the six African sub regions;**
522 **as well as country details for the three lain outliers. The unit is in MtCO₂ yr⁻¹ Shaded green areas represent the**
523 **minimum and maximum ranges from inversions. Shaded blue represents the minimum and maximum ranges**
524 **for TRENDYv9 DGVMs. Green dashes denote the mean of inversions, blue dashes denote the median of**
525 **TRENDYv9 DGVMs, green dashes the median of inversions. Positive values represent a source while the**
526 **negative values refer to a sink.**

527 For three large countries, corrected UNFCCC values from Grassi et al. show a bigger discrepancy with other
528 BU and TD methods than uncorrected ones (Fig. S9). In Namibia the corrected value gives a larger sink
529 compared to other methods, while the uncorrected value is comparable. In DRC the corrected value which
530 was a source seems a high overestimate compared to other methods, while the uncorrected UNFCCC value
531 is close to median values from inversions, and to FAO. In Nigeria, the corrected value seems to be a high
532 overestimation of a net source compared to other methods pointing to either a smaller source (FAO,
533 inversions) or even a sink (DGVM).

534 The data in Figure 5 show that most methods agree on a small net sink for African LULUCF CO₂ fluxes,
535 except for corrections following Grassi et al (2022). But disagreements exist among different methods.



536 Inversions give a smaller net sink (mean_{min}^{max}) of $-14 \frac{2966}{-2248}$ MtCO₂ yr⁻¹ than DGVMs ($-232 \frac{2095}{-1978}$ MtCO₂
 537 yr⁻¹). The median value of inversions is nevertheless within the range of DGVMs. At the scale of Africa,
 538 the inversions mean sink is ~12 times smaller than the median from DGVMs. The min-max range of
 539 inversions (5216 MtCO₂ yr⁻¹) is larger than the range of the DGVMs by 17%. DGVM and inversions show
 540 a positive temporal correlation coefficient ($r = 0.7$) for annual trends (linear fit to time series).
 541 UNFCCC values with the fourth approach point out to a net sink (-503 MtCO₂ yr⁻¹), similar to the third
 542 one. Corrected values as in Grassi et al. (2022) give a net source estimate of 265 MtCO₂ yr⁻¹. FAO net
 543 emissions and removals represent a small net source (18 MtCO₂ yr⁻¹). Differences between FAO and
 544 UNFCCC, as explained in Grassi et al. (2022), could be due to the fact that FAO estimates of CO₂ fluxes
 545 for forest remaining forest can be set to zero in absence of any national stock change inventory (Table 3).

546 **Table 3. Mean net LULUCF CO₂ (emissions and removals) over the overlapping period of the different**
 547 **datasets (2001-2018), in MtCO₂ yr⁻¹.**

Region	Corrected UNFCCC (Grassi et al. 2022) with and without DRC correction.	Corrected UNFCCC but DRC/ Nigeria/ Namibia	Median TRENDY v9	Max TREND Y v9	Min TREND Y v9	Mean GCB inv.	Max GCB inv.	Min GCB inv.	FAO total FL with FL conversion
South Africa group	-23	-23	-5	312	-368	-147	96	-418	-1
Horn of Africa	153	153	108	475	-439	-115	367	-729	-5
Southern Africa	14	141	-81	622	-785	182	1186	-548	13
North Africa	-259	-259	-13	369	-299	-34	240	-343	-9
Subsahelian West Africa	236	19	245	900	-49	-53	481	-479	21
Central Africa	144 (DRC with NDC2021) -620 (DRC with NC3)	-620	-490	461	-1051	152	1362	-1303	-1
Africa total	265 (DRC with NDC2021) -503 (DRC with NC3)	-589	-232	2095	-1978	-14	2967	-2249	-1

548 At a regional scale, we note some agreement between different bottom-up approaches. First, for the South
 549 Africa region, the mean of DGVM medians during the overlapping period 2001-2018 (-5 MtCO₂ yr⁻¹) and
 550 the FAO estimate (-1 MtCO₂ yr⁻¹) are comparable and not too far from Grassi et al., 2022 (-23 MtCO₂ yr⁻¹)
 551 ¹). Second, for North Africa, the DGVM median (-13 MtCO₂ yr⁻¹) and the FAO mean estimate over the



552 same period ($-9 \text{ MtCO}_2 \text{ yr}^{-1}$) are comparable. Finally, in Sub-Saharan West Africa, the DGVM (236
553 $\text{MtCO}_2 \text{ yr}^{-1}$) and UNFCCC corrected following Grassi et al., 2022 ($245 \text{ MtCO}_2 \text{ yr}^{-1}$) are also close to each
554 other.

555 Northern Africa is the group where DGVM and inversions point to the closest values both in terms of sign
556 (sink) and magnitudes with respectively small sinks of $-13_{-299}^{369} \text{ MtCO}_2 \text{ yr}^{-1}$ and $-34_{-343}^{240} \text{ MtCO}_2 \text{ yr}^{-1}$.

557 Looking at DGVM and inversions in the region of South Africa, we found that both DGVM and inversions
558 point to a sink (respectively $-5_{-368}^{312} \text{ MtCO}_2 \text{ yr}^{-1}$ and $-147_{-418}^{96} \text{ MtCO}_2 \text{ yr}^{-1}$), however with a different
559 magnitude. The region showing the highest discrepancies between inversions and DGVM values is Central
560 Africa with a source in inversions ($152_{-1303}^{1362} \text{ MtCO}_2 \text{ yr}^{-1}$) and a sink for DGVM ($-490_{-1051}^{461} \text{ MtCO}_2 \text{ yr}^{-1}$).
561 The Sub-Saharan West Africa also shows discrepancies in both sign and magnitude with $245_{-49}^{900} \text{ MtCO}_2$
562 yr^{-1} for DGVM and $-53_{-479}^{481} \text{ MtCO}_2 \text{ yr}^{-1}$ for inversions. The same is true for Southern Africa with
563 $-81_{-785}^{622} \text{ MtCO}_2 \text{ yr}^{-1}$ for DGVMs and $182_{-548}^{1186} \text{ MtCO}_2 \text{ yr}^{-1}$ for inversions, and the Horn of Africa
564 with $108_{-439}^{475} \text{ MtCO}_2 \text{ yr}^{-1}$ for DGVM and $-115_{-729}^{367} \text{ MtCO}_2 \text{ yr}^{-1}$ for inversions. At the regional scale, the
565 inversions systematically give smaller sinks than DGVMs in the regions of Central Africa, Sub-Saharan
566 West Africa and North Africa after 2010 (Fig. 5).

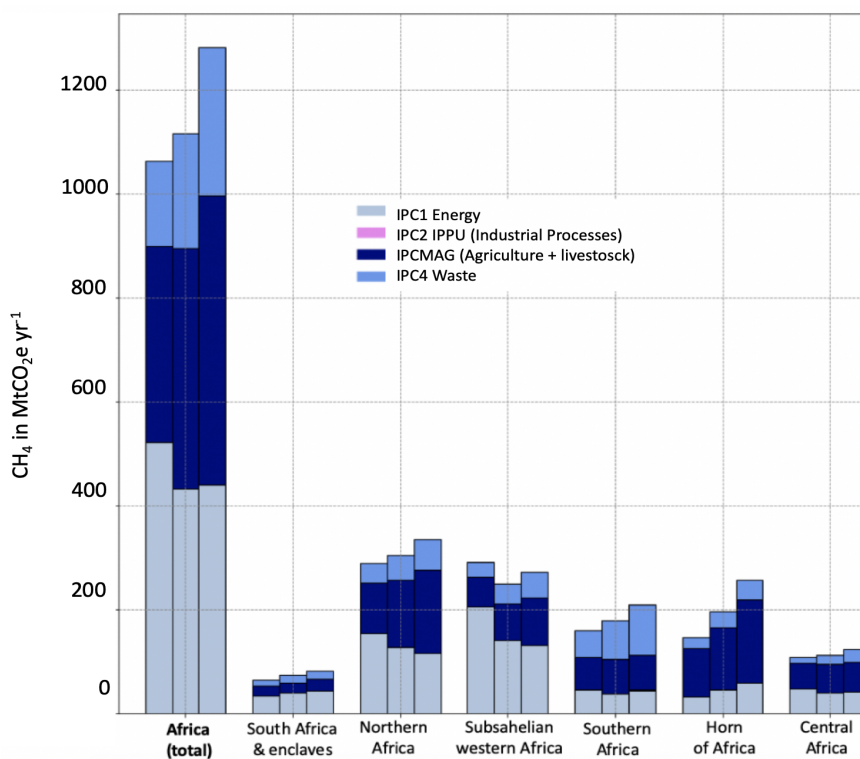
567 We also computed the coefficient of correlation at the regional level between DGVM and inversions trends
568 for each region. The highest correlation coefficients are in the South Africa region ($r = 0.7$), followed by
569 Northern Africa ($r = 0.6$) and in Southern Africa ($r = 0.5$). The lowest correlation coefficients are for the
570 group of Central African countries ($r = 0.3$), Sub-Saharan Western countries ($r = 0.2$) and the Horn of
571 Africa ($r = 0.1$).

572 2.3 CH₄ anthropogenic emissions

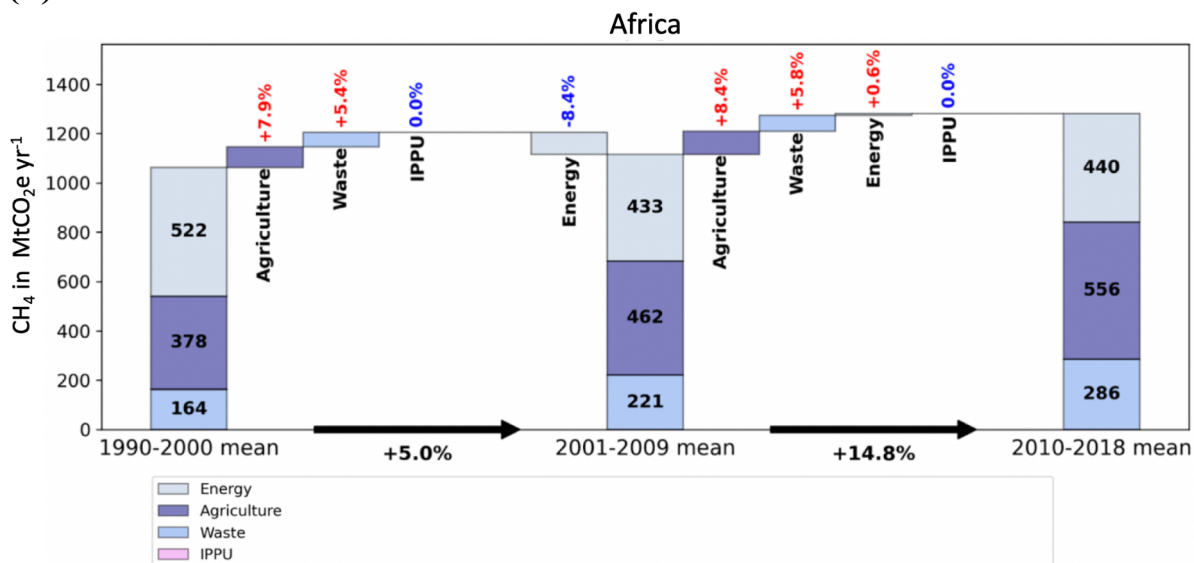
573 Total and sectoral bottom up CH₄ anthropogenic emissions and decadal changes

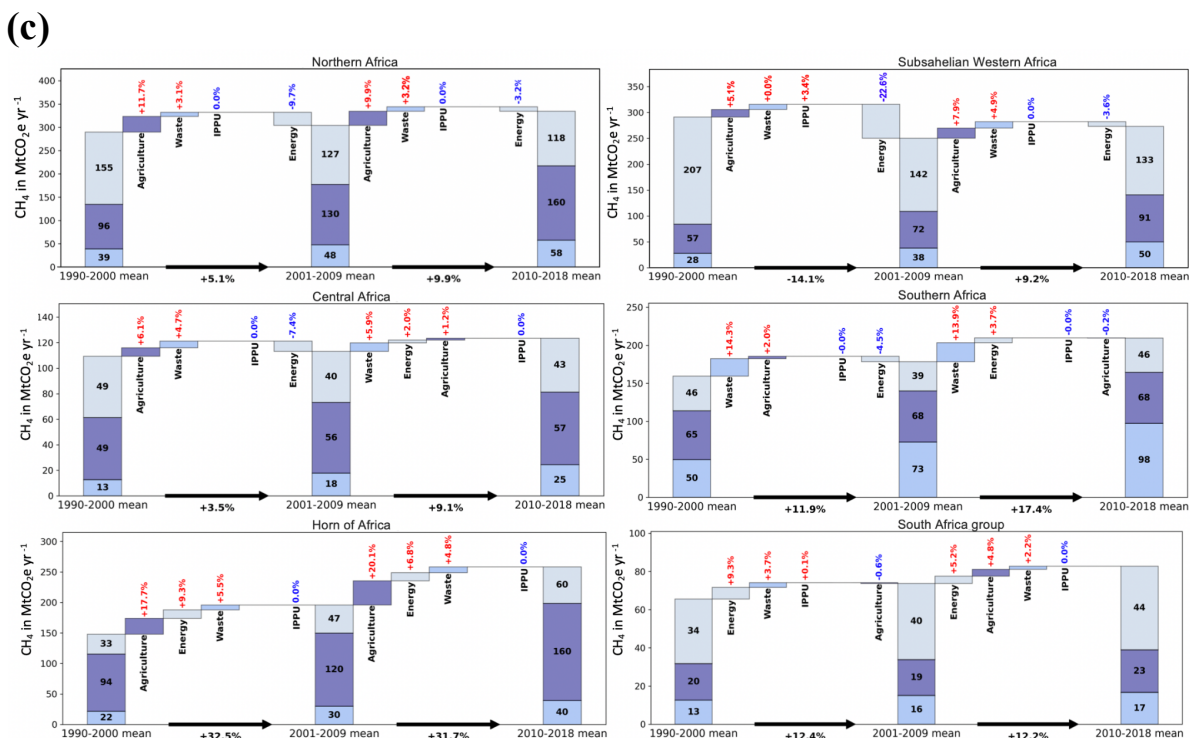


(a)



(b)





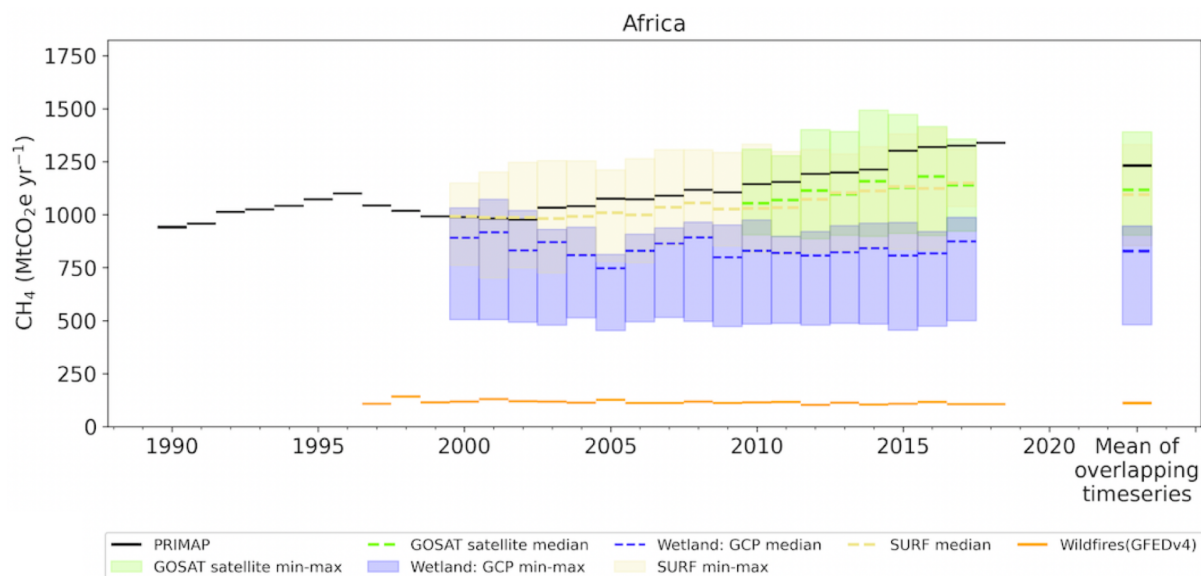
574 **Figure 6. (a) African mean anthropogenic CH₄ emissions in MtCO₂e yr⁻¹ over three decades (1990-1998, 1999-2008,**
 575 **2010-2018). (b) Contribution of each sector to the change of African emissions between the last three decades. (c)**
 576 **Same for different regions regrouping several countries. Data from PRIMAP-hist (2021).**

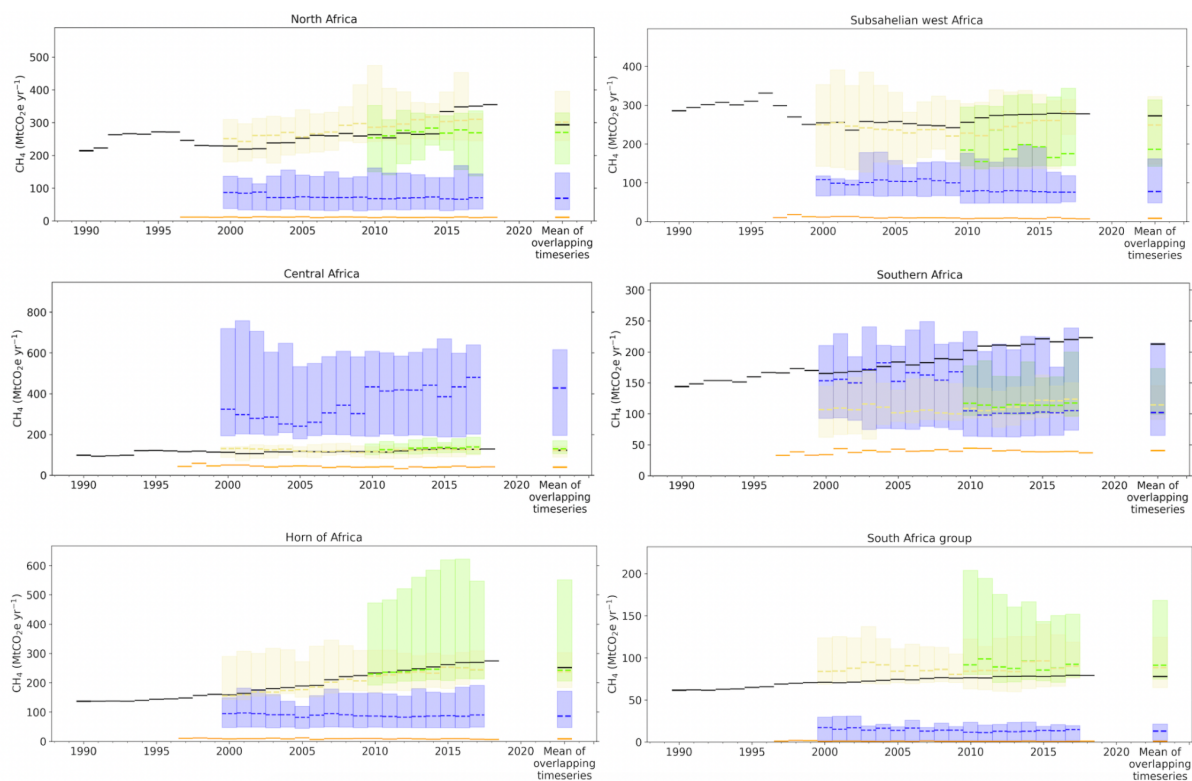
577 Figure 6 shows anthropogenic CH₄ emissions from PRIMAP-hist grouped into four super-sectors (see section
 578 1). A map of CH₄ emissions and their trends per country is given in Fig. 3c-d. LULUCF CH₄ emissions are not
 579 considered in PRIMAP-hist. African anthropogenic CH₄ emissions sum up to 1154 MtCO₂e yr⁻¹ over the last
 580 three decades. They increased from 1064 MtCO₂e yr⁻¹ in 1990-2000 to 1116 MtCO₂e yr⁻¹ in 2001-2009, and
 581 further to 1282 MtCO₂e yr⁻¹ over 2010-2018 (Fig. 6.a). Over the last three decades, the main African CH₄
 582 emitting super-sectors shifted from Energy (49% over 1990-2000) to Agriculture, mainly due to a North
 583 African contribution. At the regional level, the main contributing region to total emissions shifted over the last
 584 30 years from Sub-Saharan Western Africa (297 MtCO₂e yr⁻¹ for all sectors in 1990-2000) to North Africa
 585 (333 MtCO₂e yr⁻¹ for all sectors in 2010-2018).
 586 North African emissions increased from 290 MtCO₂e yr⁻¹ in 1990-2000 to 305 MtCO₂e yr⁻¹ in 2001-2009, and
 587 further to 333 MtCO₂e yr⁻¹ in 2010-2018. Sub-Saharan emissions decreased from 297 MtCO₂e yr⁻¹ in 1990-
 588 2000 to 252 MtCO₂e yr⁻¹ in 2001-2009, and re-increased to 274 MtCO₂e yr⁻¹ in 2010-2018, a level smaller than
 589 in the first decade (Fig. 6b). The Horn of Africa emissions increased from 149 MtCO₂e yr⁻¹ over 1990-2000, to
 590 197 MtCO₂e yr⁻¹ over 2001-2009, and further to 260 MtCO₂e yr⁻¹ over 2010-2018. The emissions from Southern



591 Africa increased from 184 MtCO₂e yr⁻¹ in 1990-2000, to 180 MtCO₂e yr⁻¹ in 2001-2009, and further to 212
592 MtCO₂e yr⁻¹ in 2010-2018. Emissions from the Central African region increased from 111 MtCO₂e yr⁻¹ in 1990-
593 2000, to 114 MtCO₂e yr⁻¹ in 2001-2009, and further to 125 MtCO₂e yr⁻¹ in 2010-2018. We also computed the
594 GINI of African countries anthropogenic CH₄ per capita emissions and obtained the following values: 0.6 in
595 1990-1998, 0.5 in 1999-2008, 0.5 in 2009-2018, thus a trend of increasing ‘inequality’ between countries. As
596 compared to per capita FCO₂ emissions, more homogeneity is observed for CH₄ per capita emissions. Similar
597 to FCO₂ emissions, the GINI values remained stable over the three decades, showing a similar level of
598 inequalities over time.

599 Bottom-up versus inversions for total and anthropogenic CH₄ emissions





600 **Figure 7. Comparison of total anthropogenic CH₄ emissions in MtCO₂e yr⁻¹ from the PRIMAP-hist inventory**
 601 **(black) and global inversions. Shaded green and yellow areas represent the minimum and maximum range from**
 602 **GOSAT satellite and surface inversions, respectively. Shaded blue areas represent the minimum and maximum**
 603 **ranges of wetlands natural emissions from inversions. The orange lines represent wildfire emissions from GFED4.**

604 Figure 7 compares bottom-up anthropogenic emissions from PRIMAP-hist for the period 2000–2018 with
 605 inversions’ anthropogenic emissions (see section 1). Wetlands natural emissions are shown in the figure only
 606 for information from the median and range of inversions. Over the overlapping time period, medians of both
 607 GOSAT and surface inversions are always smaller than PRIMAP-hist emissions, at continental and regional
 608 level, except for the Central African region. For the African continent, the mean and min-max of GOSAT
 609 inversions for anthropogenic CH₄ emissions over 2000–2018 is 1117_{903}^{1390} MtCO₂e yr⁻¹, very close to the mean
 610 of surface inversions of 1094_{853}^{1330} MtCO₂e yr⁻¹. A good agreement between GOSAT and surface inversions was
 611 also found in other high-emitting countries (Deng et al., 2021). In contrast, PRIMAP-hist gives a mean of CH₄
 612 anthropogenic emissions of 1231 MtCO₂e yr⁻¹ over the period 2010–2017. The mean wetlands flux from
 613 inversions over 2010–2017 is of 827_{481}^{946} MtCO₂e yr⁻¹. Methane emissions from wildfires over Africa for the
 614 same period are less important, with a mean of 110 MtCO₂e yr⁻¹.



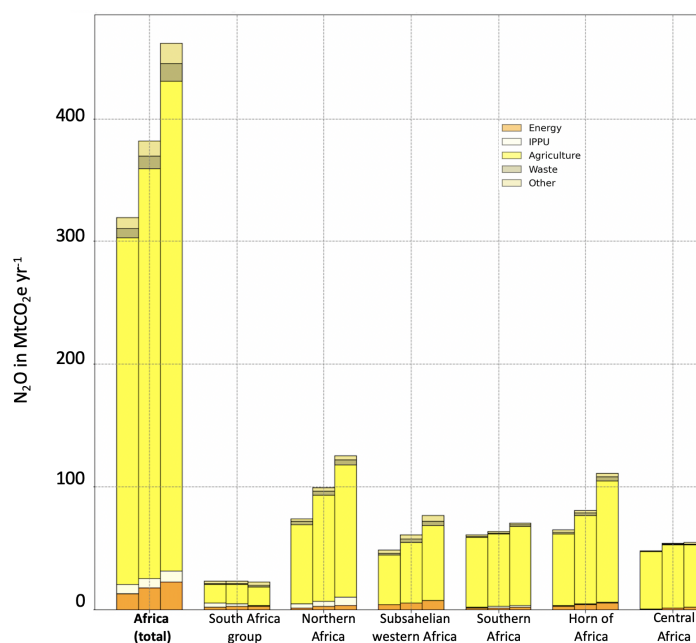
615 Regional emissions from PRIMAP-hist ranked in decreasing order are: North Africa (293 MtCO₂e yr⁻¹) > Sub-
616 Sahelian west Africa (272 MtCO₂e yr⁻¹) > Horn of Africa (252 MtCO₂e yr⁻¹) > Southern Africa (212 MtCO₂e
617 yr⁻¹) > Central Africa (123 MtCO₂e yr⁻¹) > South Africa (78 MtCO₂e yr⁻¹). For both GOSAT and surface
618 inversions, the ranking of regions (Table S10) is almost the same for surface inversions and PRIMAP-hist, with
619 the exception of Central Africa and Southern Africa.

620 2.4 Results for N₂O emissions

621 N₂O PRIMAP-hist versus atmospheric inversions (total flux)

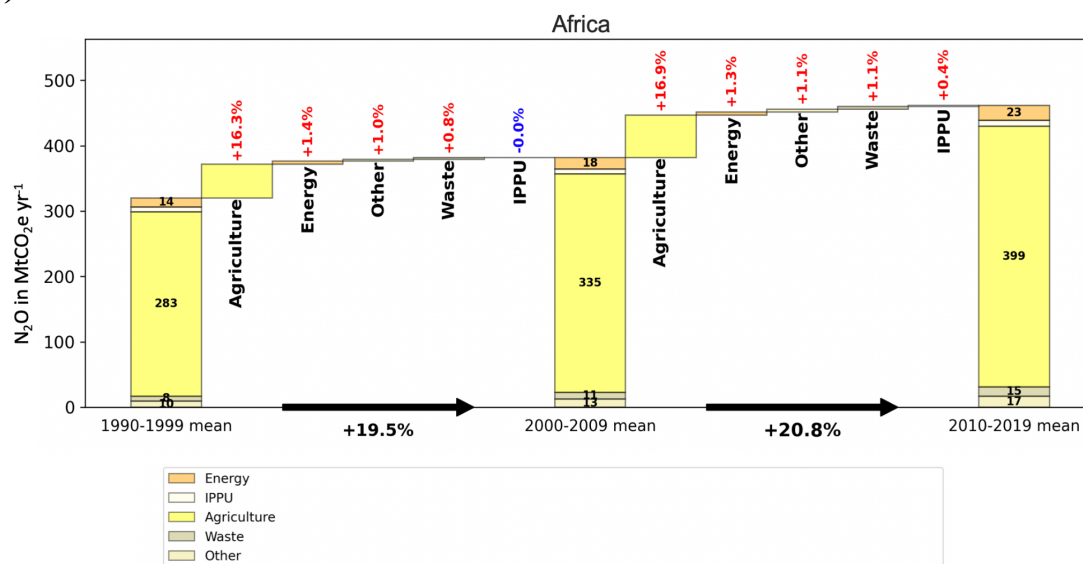
622 Total and sectoral N₂O anthropogenic emissions (PRIMAP-hist)

(a)

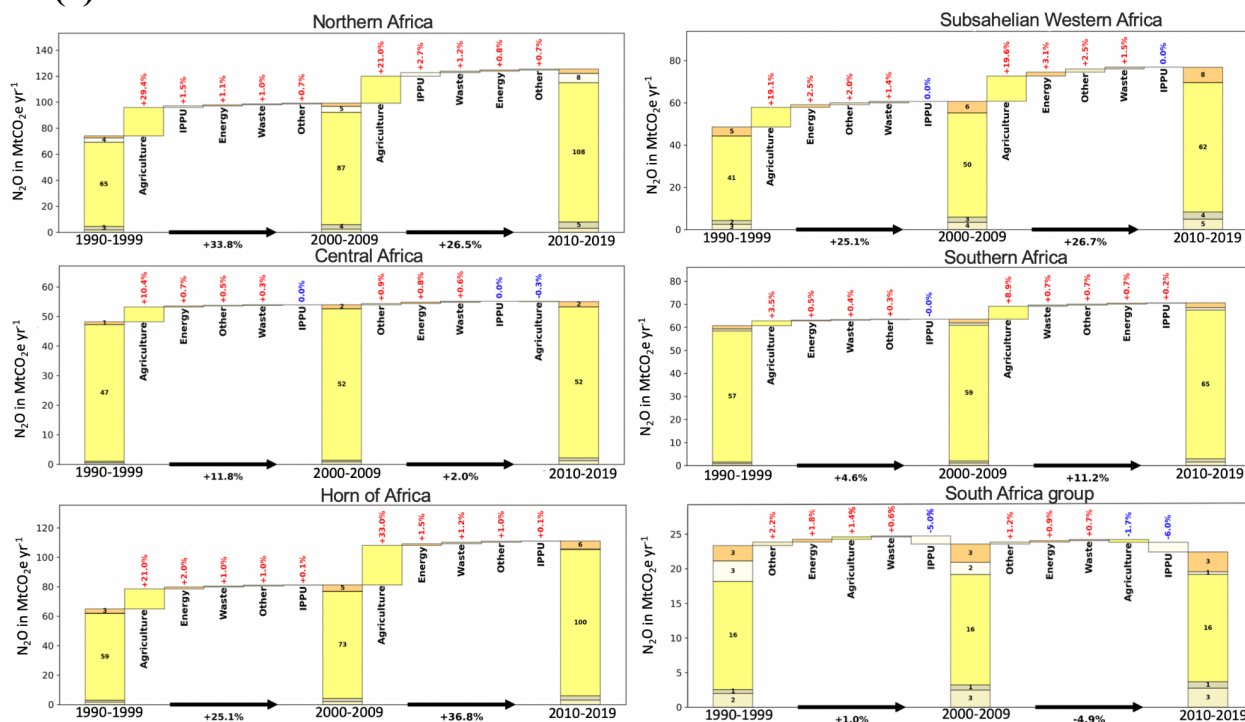




(b)



(c)



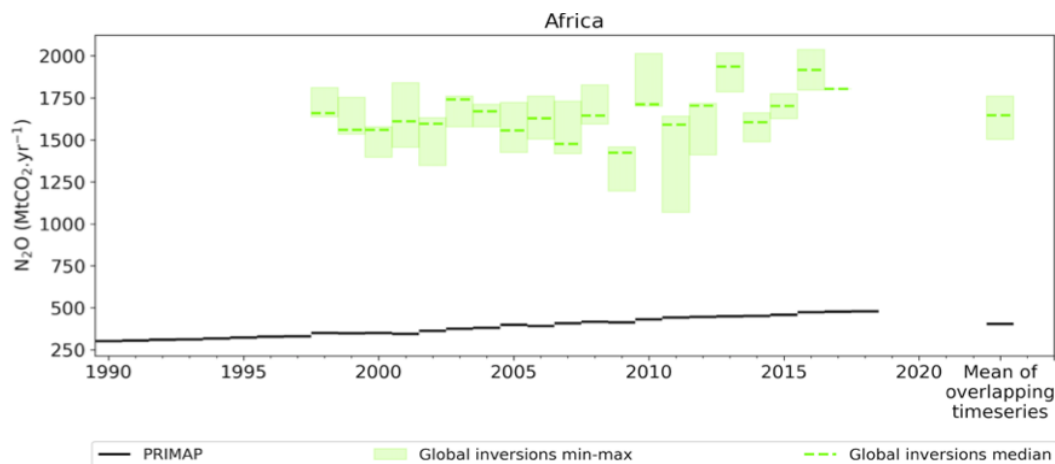
623 **Figure 8. (a) African anthropogenic N₂O emissions in MtCO₂e yr⁻¹ over three decades: 1990-1998, 1999-2008 &**
 624 **2009-2019. Data from PRIMAP-hist (2021). (b) Contribution of each sector to the change of African N₂O emissions**

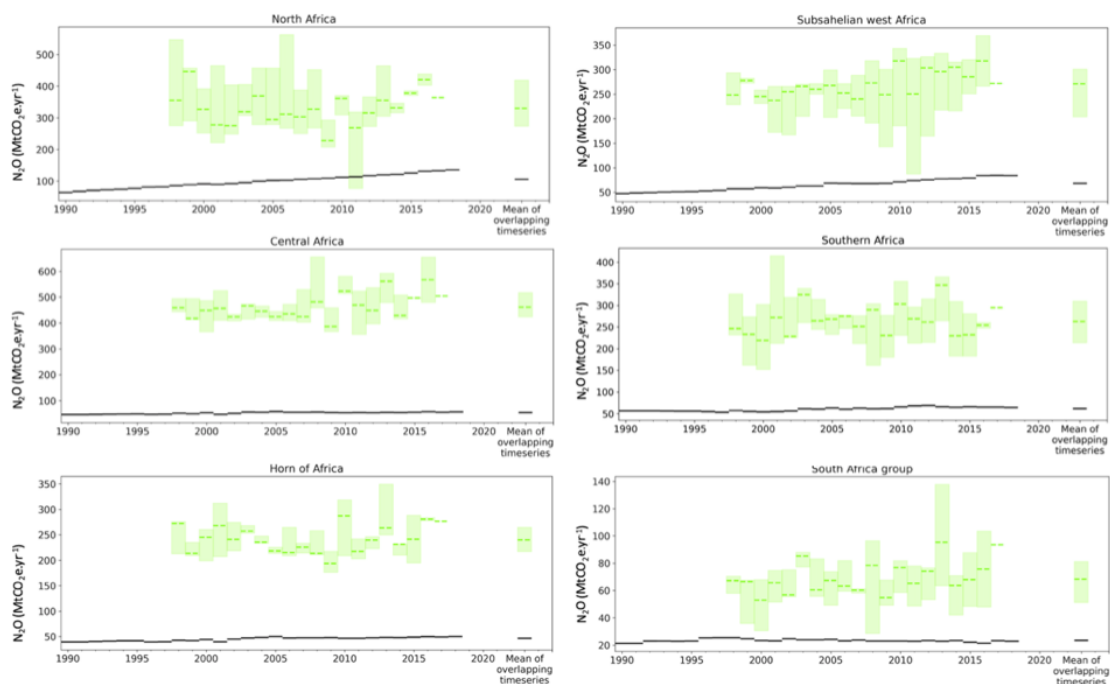


625 between the last three decades. (c) Same for different regions regrouping several countries. Data from PRIMAP-
626 hist (2021).

627 Figure 8 presents anthropogenic N₂O emissions from PRIMAP-hist, for five sectors (for country values, see
628 Fig. 4). Over the last three decades, the mean African emissions are 378 MtCO₂e yr⁻¹, three times less than CH₄
629 emissions. The mean decadal N₂O emissions increased from 319 MtCO₂e yr⁻¹ in 1990-1999, to 382 MtCO₂e yr⁻¹
630 ¹ in 2000-2009 (+20%), and further to 431 MtCO₂e yr⁻¹ in 2010-2018. Over the last three decades, the main
631 emitting sector remained Agriculture. The N₂O emissions increase also originates from Agriculture, with an
632 increase from 283 MtCO₂e yr⁻¹ to 335 MtCO₂e yr⁻¹ between 1990-1999 and 2000-2009, that is, +16.3 %
633 compared to of the total emission increase of +19.5%. The three other sectors show a smaller contribution to
634 the emissions increase: Energy (+1.4%), Other (+1%) and Waste (+0.8%). IPPU shows no change. Similarly,
635 between 2000-2009 and 2010-2019, the N₂O emissions increase also came from the sector of Agriculture, with
636 an increase from 335 MtCO₂e yr⁻¹ to 399 MtCO₂e yr⁻¹ between 1990-1999 and 2000-2009.

637 The main contributing regions to the continental emissions are Northern Africa and the Horn of Africa (Fig.
638 8a). Between 2000-2009 and 2010-2019, the North African contribution increased from 99 MtCO₂e yr⁻¹ to 125
639 MtCO₂e yr⁻¹ (+27%). The main sectoral contribution is always Agriculture, which increased in that region from
640 86 MtCO₂e yr⁻¹ to 107 MtCO₂e yr⁻¹ (+21%). Emissions from the second largest emitting region, the Horn of
641 Africa, increased from 81.19 MtCO₂e yr⁻¹ in 2000-2009 to 111 MtCO₂e yr⁻¹ in 2010-2019 (+37%), mainly from
642 Agriculture. In the third most emitting region, Sub-Saharan Africa, emissions increased from 61 MtCO₂e yr⁻¹
643 in 2000-2009 to 77 MtCO₂e yr⁻¹ in 2010-2019 (+27%), also from Agriculture. The least contributing region to
644 the increase of the total N₂O emissions from 2000-2009 to 2010-2019 is South Africa which had a very small
645 decrease, mainly from IPPU (-6%) followed by Agriculture (-2%). On the contrary, there is a slight increase of
646 N₂O emissions for the group of South Africa for the Other (+1%), Energy (+1%) and Waste (+1%) sectors.





647 **Figure 9. Total N₂O emissions from PRIMAP-hist in MtCO₂e yr⁻¹ (black line) from three GCP atmospheric**
 648 **inversions for the entire African continent and for six African sub-regions. The green line is the median of the three**
 649 **inversions and the light green areas the maximum-minimum range.**

650 Figure 9 compares N₂O emissions from PRIMAP-hist and inversions. For total Africa, the mean of inversions
 651 emissions over the overlapping time period 1998-2017 is 1647_{1502}^{1760} MtCO₂e yr⁻¹, much larger than the
 652 PRIMAP-hist estimate of 360 MtCO₂e yr⁻¹. According to PRIMAP-hist, total African emissions increased by
 653 28% between 1998 and 2017, while the trend of emissions from the inversions is $16 \pm 8\%$. At regional scale,
 654 emissions from inversions ranked in decreasing order are: Central Africa (461_{424}^{517} MtCO₂e yr⁻¹) > North Africa
 655 (330_{274}^{419} MtCO₂e yr⁻¹) > Sub-Saharan West Africa (271_{68}^{330} MtCO₂e yr⁻¹) > Southern Africa (263_{214}^{310} MtCO₂e
 656 yr⁻¹) > Horn of Africa (240_{217}^{265} MtCO₂e yr⁻¹) > South Africa (68_{51}^{81} MtCO₂e yr⁻¹). According to PRIMAP-hist, the
 657 ranking is: North Africa (106 MtCO₂e yr⁻¹) > Sub-Saharan West Africa (68 MtCO₂e yr⁻¹) > Southern Africa
 658 (62 MtCO₂e yr⁻¹) > Central Africa (54 MtCO₂e yr⁻¹) > the Horn of Africa (46 MtCO₂e yr⁻¹) > South Africa (24
 659 MtCO₂e yr⁻¹) (See also Table S12). Emissions from PRIMAP-hist are smaller than inversions by a factor of 16.
 660 This is likely due to the fact that we did not attempt to separate natural from anthropogenic emissions in
 661 inversions. Other studies (Ciais et al., 2021; Petrescu et al., 2021 in Europe) showed that even after subtracting
 662 N₂O natural estimates, inversions always point to higher estimates than BU methods.

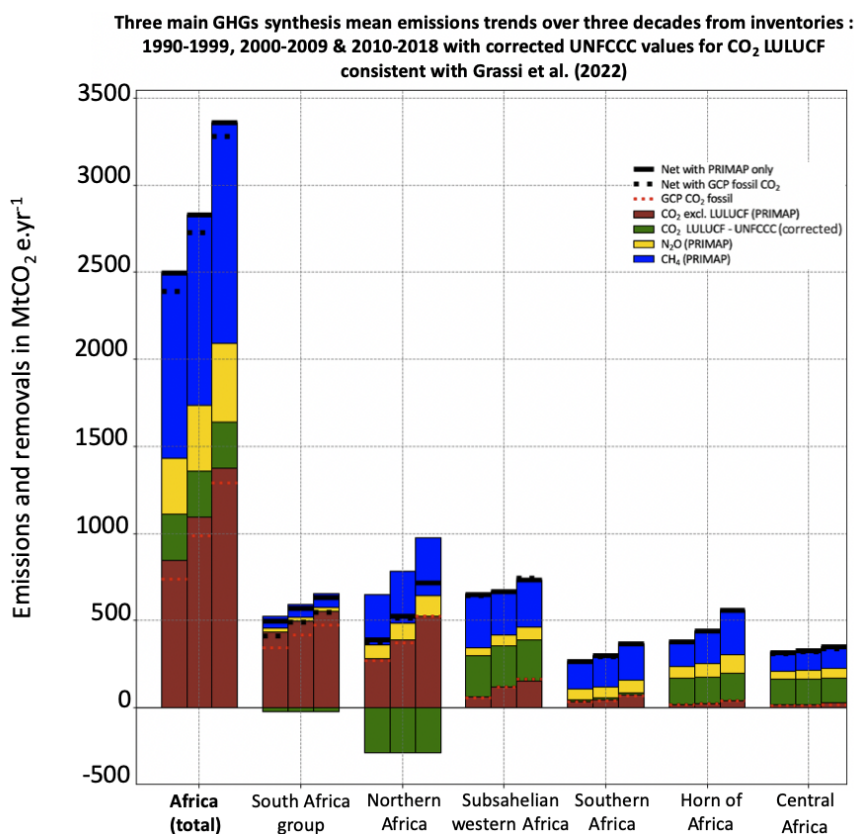
663 **3 Discussion: synthesis for the three main GHG and comparison between BU and TD methods**



664 3.1 Synthesis of the steps for assessing net GHG trends over Africa

665 Here, we propose a first step towards the elaboration of what could become a more systematic method for a
666 scientific benchmark of non-Annex I national inventories: 1) correct outliers, 2) a discussion about the
667 realisms of estimates including considering geophysical aspects, 3) a proposal of an independent evaluation
668 of inventory data by experts, 4) a comparison between UNFCCC data corrected thanks to expert judgment
669 and other BU and TD methods, 5) computation of the mean of all BU and TD methods, 6) computation of
670 “best fitted BU values” (meaning “best fitted BU values” excluding uncorrected UNFCCC data), and “TD
671 values” (meaning “best fitted TD values”: without considering N₂O inversions replaced with PRIMAP-hist
672 values), 7) identification of ranking anomalies.

673 3.2 Net GHG budget from bottom-up estimates



674 Figure 10. Synthesis for the three main GHG from inventories (after UNFCCC LULUCF CO₂ corrections
675 consistent with Grassi et al. (2022)) for the three main GHG with net African budget computation by BU inventories
676 for Africa as a whole and for six sub-groups of African countries across three different decades (1990-1999, 2000-



677 2010, 2010-2018) using data and corrections from country inventories. Following the atmospheric convention,
 678 positive numbers represent an emission to the atmosphere and the negative values represent a sink. Black
 679 horizontal lines represent a net flux resulting from the addition of the three main GHG using PRIMAP-hist only,
 680 dashed black horizontal lines also represent the net flux resulting from the addition of the three main GHG but
 681 using the GCP dataset for FCO₂. Dashed red lines represent the fluxes from GCP FCO₂ available in the most recent
 682 GCP paper, to compare them with PRIMAP-hist results which are represented with the brown bar plots. The N₂O
 683 and CH₄ fluxes from PRIMAP-hist are respectively represented with yellow and blue bars. CO₂ emissions and
 684 sinks from LULUCF are represented in green, they are taken from NC/BUR UNFCCC datasets with corrections
 685 applied. Unit is MtCO₂e yr⁻¹.

686 Figure 10 shows the budget for the three GHG from UNFCCC data with LULUCF data corrected using the
 687 second approach. There is a clear increase of African total GHG emissions during the last 3 decades. The
 688 differences between bottom-up datasets are mainly due to different sectoral allocations. However, the trends
 689 are consistent and comparable, and differences among inventories tend to be less for the most recent decade.

690 **Table 5. Mean net total Africa and regional groups' emissions and removals from BU methods using either GCP**
 691 **or PRIMAP-hist for FCO₂ over 2001-2017 in MtCO₂e.yr⁻¹.**

Region	BU methods with GCP FCO ₂					BU methods with PRIMAP FCO ₂				
	GCP + uncorrected UNFCCC LULUCF CO ₂	GCP + corrected UNFCCC LULUCF CO ₂ as Grassi et al. (2022)	GCP + corrected UNFCCC LULUCF CO ₂ as Grassi et al. (2022) but for DRC, NAM, NIG	GCP + median TRENDY v9 LULUCF CO ₂ (min/max)	GCP + LULUCF CO ₂ FAO total FL	PRIMAP + uncorrected UNFCCC LULUCF CO ₂	PRIMAP + corrected UNFCCC LULUCF CO ₂ as Grassi et al. (2022)	PRIMAP + corrected UNFCCC LULUCF CO ₂ as Grassi et al. (2022) but for DRC, NAM, NIG	PRIMAP + median TRENDY v9 LULUCF CO ₂ (min/max)	PRIMAP + LULUCF CO ₂ FAO total FL
Africa total	-599	2975	2122	2478 ⁴⁸⁰⁶ ₇₃₂	2728	-502	3069	2216	2572 ⁴⁸⁹⁹ ₈₂₇	2822
North Africa	613	589	589	835 ¹²¹⁶ ₅₄₉	839	620	597	597	842 ¹²²⁴ ₅₅₇	846
Central Africa	-2605	316	-448	-318 ⁶³³ ₋₈₇₉	171	-2598	324	-440	-310 ⁶⁴¹ ₋₈₇₁	179
Subsahelian West Africa	19	718	501	726 ¹³⁸² ₄₃₃	503	15	714	497	723 ¹³⁷⁸ ₄₃₀	500
Southern Africa	149	346	473	251 ⁹⁵³ ₋₄₅₃	345	151	347	475	252 ⁹⁵⁵ ₋₄₅₂	346
South Africa group	640	524	524	542 ⁸⁶⁰ ₁₇₉	546	719	603	603	621 ⁹³⁹ ₂₅₈	625
Horn of Africa	586	484	484	438 ⁸⁰⁵ ₋₁₀₉	325	587	484	484	439 ⁸⁰⁶ ₋₁₀₈	326



692 At the country level, a small number of countries showed an increasing difference between PRIMAP-hist and
693 GCP estimates of fossil CO₂ emissions over time, but they are small FCO₂ emitters. The differences may also
694 be partly explained by changes in accounting methods as mentioned in Gütschow et al. (2016). The biggest
695 discrepancies are noticeable for Mali (64%), Cameroon (-62%), and the DRC (-38%), but those three countries
696 are not major FCO₂ emitters (Fig. 4.a-b).

697 Table 5 shows the differences of net African budget from various BU methods using GCP or PRIMAP-hist for
698 FCO₂ over 2001-2017 that are also illustrated on Fig. 11.

699 **Bottom-up LULUCF budget from UNFCCC corrected by Grassi**

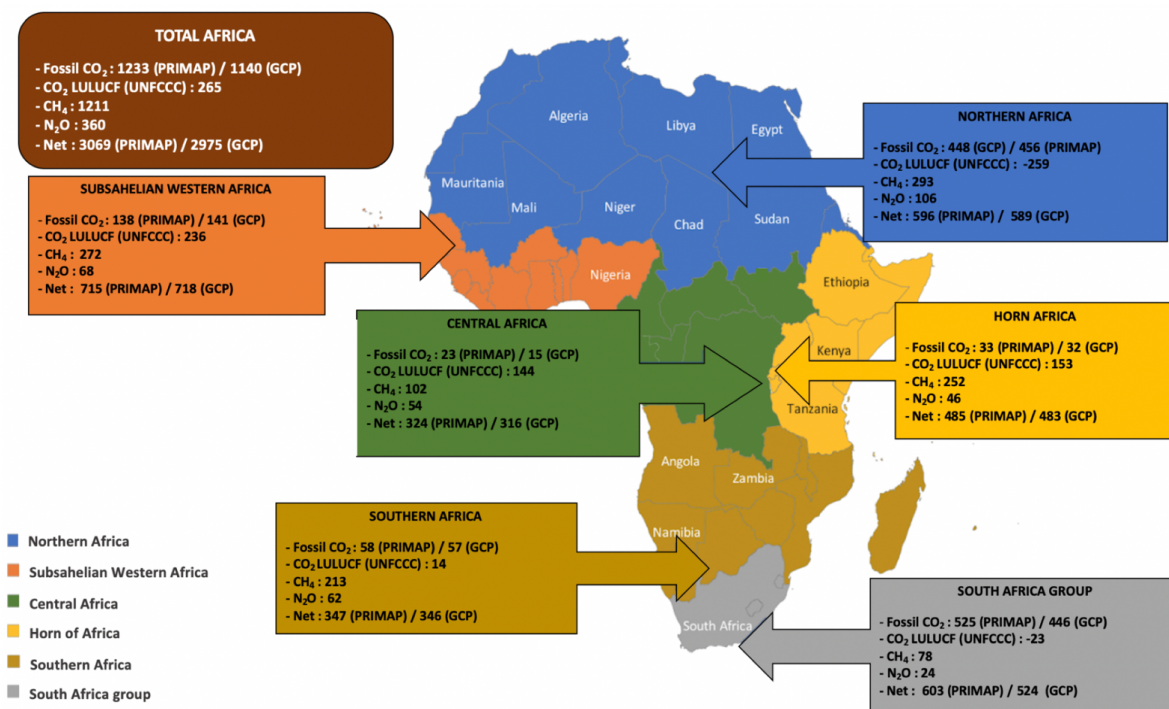
700 Over 2001-2017 the net bottom-up GHG budget is 2975 MtCO₂e yr⁻¹. Regionally the ranking in decreasing
701 order is: Sub-Saharan West Africa (718 MtCO₂e yr⁻¹) > North Africa (588 MtCO₂e yr⁻¹) > South Africa group
702 (524 MtCO₂e yr⁻¹) > Horn of Africa (484 MtCO₂e yr⁻¹) > Southern Africa (346 MtCO₂e yr⁻¹) > Central Africa
703 (316 MtCO₂e yr⁻¹).

704 **Bottom-up LULUCF budget CO₂ from FAO**

705 The bottom-up budget from FAO data is 2728 MtCO₂e yr⁻¹, 8% less than above. The ranking of regions in
706 decreasing order is: North Africa (838 MtCO₂e yr⁻¹) > South Africa group (546 MtCO₂e yr⁻¹) > Sub-Saharan
707 West Africa (503 MtCO₂e yr⁻¹) > Southern Africa (345 MtCO₂e yr⁻¹) > Horn of Africa (325 MtCO₂e yr⁻¹) >
708 Central Africa (171 MtCO₂e yr⁻¹).

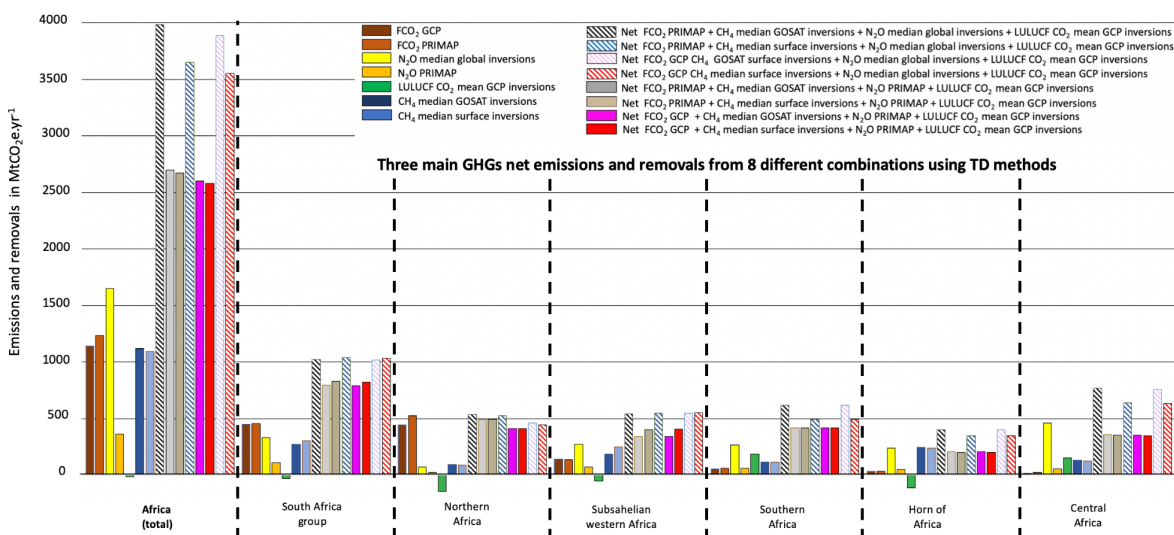
709 **Bottom-up LULUCF budget from DGVMs**

710 The net GHG budget for Africa is of 2478 $\frac{4806}{733}$ MtCO₂e yr⁻¹ MtCO₂e yr⁻¹, 9% less than with FAO. The ranking
711 of regions in decreasing order is: North Africa (835 $\frac{1216}{549}$ MtCO₂e yr⁻¹) > Sub-Saharan West Africa
712 (726 $\frac{1382}{433}$ MtCO₂e yr⁻¹) > South Africa (542 $\frac{859}{179}$ MtCO₂e yr⁻¹) > Horn of Africa (438 $\frac{805}{-109}$ MtCO₂e yr⁻¹) >
713 Southern Africa (251 $\frac{953}{-453}$ MtCO₂e yr⁻¹) > Central Africa (-318 $\frac{633}{-879}$ MtCO₂e yr⁻¹).



714 **Figure 11.** 2001-2018 emissions in MtCO₂e yr⁻¹ for fossil CO₂ (GCP and PRIMAP-hist), LULUCF CO₂ (corrected
 715 UNFCCC data consistent with Grassi et al. (2022), CH₄ (PRIMAP-hist), N₂O (PRIMAP-hist) for Africa, and for
 716 six regions.

717 **3.3 Net GHG budget from inversions**

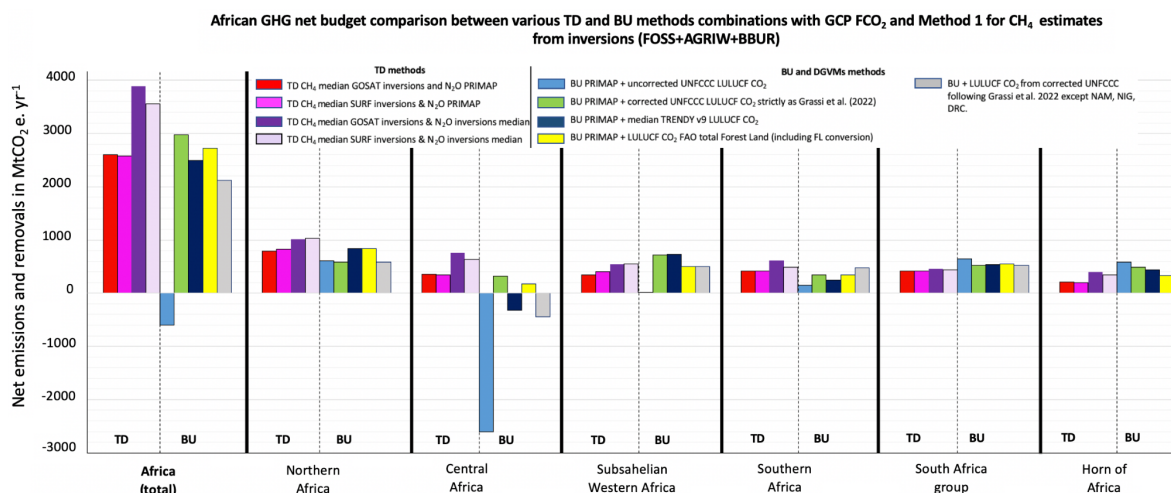




718 **Figure 12. Synthesis for the three main GHG with net African budget computation by all TD methods for Africa**
 719 **as a whole and for six sub-groups of African countries across overlapping time series (2001–2017). Following the**
 720 **atmospheric convention, positive numbers represent an emission to the atmosphere and the negative values**
 721 **represent a sink. The CO₂ emissions and sinks from LULUCF are represented in green, they are taken from GCP**
 722 **2020 dataset. Unit is MtCO₂e yr⁻¹.**

723 Figure 12 shows different combinations of inversion GHG budgets and individual gasses contributions.
 724 For total Africa, the mean net GHG budget from inversions where N₂O inversions are replaced by PRIMZP-
 725 hist is 2638 $\frac{5873}{1761}$ MtCO₂e yr⁻¹, differing only by 1 % from the bottom up GHG budget. Regional GHG budgets
 726 in decreasing order are: North Africa (810 $\frac{1170}{279}$ MtCO₂ yr⁻¹) > South Africa group (452 $\frac{751}{161}$ MtCO₂ yr⁻¹) >
 727 Southern Africa (416 $\frac{1465}{334}$ MtCO₂ yr⁻¹) > Sub-Saharan West Africa (373 $\frac{1051}{36}$ MtCO₂ yr⁻¹) > Central Africa
 728 (352 $\frac{1592}{1133}$ MtCO₂ yr⁻¹) > Horn of Africa (204 $\frac{873}{456}$ MtCO₂ yr⁻¹) (Table S16). The mean net of inversions
 729 including N₂O inversions is substantially higher, 3879 $\frac{7341}{1320}$ MtCO₂e yr⁻¹. Regional GHG budgets in decreasing
 730 order are: North Africa (1034 $\frac{1475}{600}$ MtCO₂e yr⁻¹) > Central Africa (759 $\frac{2054}{763}$ MtCO₂e yr⁻¹) > Southern Africa
 731 (616 $\frac{1713}{262}$ MtCO₂e yr⁻¹) > Sub-Saharan West Africa (576 $\frac{1313}{61}$ MtCO₂e yr⁻¹) > South Africa group
 732 (496 $\frac{814}{138}$ MtCO₂e yr⁻¹) (Table S16).

733 3.4 Comparison between bottom-up and top-down methods



734 **Figure 13. Synthesis for the three main GHG net African budget from TD and BU methods. using Method 1**
 735 **regarding anthropogenic CH₄ estimated from inversions (FOSS+AGRIW+BBUR) for comparative net emissions**
 736 **and removals computation by BU and TD methods for Africa as a whole and for six sub-groups of African countries**
 737 **across the overlapping period (2001–2017). FCO₂ data from GCP. N₂O from global inversions and from PRIMAP-**
 738 **hist. For TD methods, anthropogenic CH₄ from both GOSAT and surface inversions are used, and LULUCF from**



739 **GCP inversions only. For BU methods, anthropogenic CH₄ and N₂O from PRIMAP are used, and with five different**
740 **methods for assessing LULUCF CO₂: from uncorrected UNFCCC data; from corrected UNFCCC data according**
741 **Grassi et al. (2022); from corrected UNFCCC except Namibia, Nigeria and DRC; from TRENDY v9; from FAO**
742 **FL including FL conversions. Following the atmospheric convention, positive numbers represent an emission to**
743 **the atmosphere and the negative values represent a sink. All values are in MtCO₂e.**

744 Figure 13 shows the GHG budgets from all combinations of bottom-up and top-down methods. The mean of
745 all methods after filtering outliers (Grassi et al. (2022) UNFCCC corrections, using PRIMAP instead of
746 inversions for N₂O) is 2630 $\frac{4557}{1974}$ MtCO₂e yr⁻¹, which represents only % of global FCO₂ emissions. The mean
747 of all estimates points out to a source in the six African regions ranked in decreasing order as: North Africa
748 (761 $\frac{988}{460}$ MtCO₂e yr⁻¹) > South Africa group (513 $\frac{702}{161}$ MtCO₂e yr⁻¹) > Horn of Africa (318 $\frac{699}{80}$ MtCO₂e yr⁻¹) >
749 Sub-Saharan West Africa (492 $\frac{913}{286}$ MtCO₂e yr⁻¹) > Southern Africa (354 $\frac{998}{78}$ MtCO₂e yr⁻¹) > Central Africa
750 (143 $\frac{882}{670}$ MtCO₂e yr⁻¹).

751 **3.5 Uncertainties specific to DGVM / inversions for LULUCF CO₂**

752 In Fig. 5, we showed important disagreements among models regarding LULUCF CO₂ on whether Africa has
753 been a small source over the last 20 years (as shown by inversions) or a net sink (as shown by DGVM and
754 UNFCCC except with the Grassi et al. correction). There is also more interannual variability in the DGVM
755 results, mainly from climate, which is absent from UNFCCC as inventories provide only decadal smoothed
756 flux estimates. The larger sink in the DGVM compared to the corrected UNFCCC estimates using the method
757 of Grassi et al. (2022) may be due to the fact that non-Annex I UNFCCC estimates generally do not include
758 dead biomass or harvested wood products. If forest biomass is estimated by a stock-change approach,
759 therefore, changes in living biomass due to transfer to dead biomass and harvested wood products will be
760 considered emitted in that year, while in the DGVM it will decay more slowly over time. Another difference
761 is the treatment of land use change emissions, based on historical global land use change maps for the DGVM,
762 which can significantly differ from national land use datasets. On the other hand, DGVM do not represent
763 forestry and may underestimate sinks in intensively managed young forests. Finally, DGVM do not separate
764 between unmanaged and managed lands, while UNFCCC inventories only account for managed land, yet
765 including conservation areas and indigenous territories. Grassi et al. (2022) showed that the difference
766 between the global UNFCCC sink (1100 MtCO₂ yr⁻¹) and the global land carbon sink (4767 MtCO₂e yr⁻¹)
767 must be explained by the contribution of non-managed lands. But in the case of Africa, it was not possible to
768 extract from UNFCCC reports the national areas of unmanaged land, and we had to also look at UNFCCC
769 Technical Assessment Reports (TAR) as well as REDD+ reports to extract information. Methods of
770 assessment have not been fully standardized since 1990, and they differ depending on the countries analyzed,



771 and on the emissions categories considered. In this context, when comparing UNFCCC estimates with data
772 from DGVM and inversion models, different layers of aggregated uncertainties affect the analysis. (Deng et
773 al., 2021; Petrescu et al., 2021; Grassi et al., 2018).

774 **3.6 Differences between bottom-up and top-down CH₄ emissions**

775 The methodology used for removing natural CH₄ emissions from inversions is key for comparing with bottom-
776 up estimates. In this paper, we used a separation based on the natural emissions solved by each inversion
777 (section 2.3 method 1). Using an alternative method from Deng et al. (2022) based on natural emissions from
778 the median of all inversions gives smaller anthropogenic emissions than PRIMAP-hist (Fig. S10).

779 **3.7 Differences between bottom-up and top-down N₂O emissions**

780 For N₂O emissions, discrepancies between inventories and inversions are very high, especially for the group of
781 Central African countries, where the vegetation covers an important land area with likely large natural N₂O
782 (Deng et al., 2022). We can suppose that more broadly for all African groups, the lack of accounting of natural
783 emissions is the main reason why PRIMAP-hist estimates are much smaller than inversions. All African
784 countries used Tier 1 emission factors and include only direct N₂O emissions. The study by Deng et al. (2022)
785 underlined that indirect anthropogenic emissions notably coming from “atmospheric nitrogen deposition and
786 leaching from anthropogenic nitrogen additions to aquifers and inland water are usually not reported by non-
787 Annex I countries” and that this under-reported source of anthropogenic emissions tends to represent about 5%
788 to 10% of anthropogenic N₂O.

789 **4 Summary, concluding remarks and perspectives**

790 Africa is a large continent gathering 56 countries, and some countries are major GHG emitters. Because of its
791 rapidly growing population and high industrial potential, Africa is a critical geography regarding climate
792 change mitigation and adaptation policy. Depending on the emissions pathways, Africa, which is already a big
793 emitting region, is expected to represent between at least a bit more than 10% of the global share by 2050, and
794 could become as high as 18% of global emissions by 2050 (van der Zwaan, 2018).

795 This paper delivers both a continental view and a detailed analysis of the three main GHG trends during the
796 last thirty years across this continent as a whole, across relevant groups of countries given the inversions’
797 resolutions, and also considering country details. Thanks to the comparison of different methods and datasets,
798 the uncertainty about the net emissions and removals of GHG lowers. The interest of studying Africa is high
799 not only from a scientific point of view, but also from a climate-policy perspective, as under the UNFCCC



800 principle of “common but differentiated responsibility” about global warming, the credibility of the PA lies in
801 the effective participation and inclusiveness of all parties, including non-Annex I countries. Our effort of
802 comparing BU datasets and inversions and analyzing differences for African GHG emissions and removals
803 assessment by looking at trends since 1990 will also be useful for future updates on a regular basis within the
804 2023 GST perspective.

805 At the scale of Africa, there is a rapid increase of FCO₂ emissions that roughly doubled since 1990. This increase
806 is dominated by coal emissions for the decade 1990-1998 compared to 1999-2008 (+9%), and by oil for the
807 decade 1999-2008 compared to the decade 2008-2017 (+16%). As for CO₂ LULUCF, we found that BU
808 estimates are featured with important annual fluctuations, as opposed to periodic national inventories
809 assessments, the reconciliation between the sectoral classification for anthropogenic estimates between TD and
810 BU has to be done “manually” and is not uniform to date, which doesn’t facilitate the comparability of those
811 different approaches. There are also differences among GCP inversions for CO₂, due to the fact that choices of
812 model transport may differ among models, because prior fluxes can also differ between modeling teams, and
813 because the African GHG observation network is featured with few stations and relatively scarce data. The lack
814 of integration of CO₂ lateral anthropogenic and river fluxes is also an issue to be taken into account when trying
815 to compare BU and TD methods (Ciais et al., 2022), and in the present study we did integrate those lateral
816 fluxes. Anthropogenic CH₄ from PRIMAP-hist estimates indicate that out of the total African emissions
817 increase from 1064 MtCO₂e yr⁻¹ to 1116 MtCO₂e yr⁻¹ between 1990-2000 and 2001-2009 (+5%), only two
818 sectors contributed: Agriculture, in a dominant way (+8%) and Waste (+5%). Energy contributes to emissions
819 decrease (-8%) that is however too small to offset other sectors’ CH₄ emissions that represent a net increase.
820 The main regional contributions come from North Africa and from the Agriculture sector (+12%). Over the
821 same period, the least contributing emitter is the group of South Africa (+12%), with only one decreasing
822 emissions sector: Agriculture (-1%). The mean 2001-2009 emissions increased by +15% over 2010-2018 with
823 contribution from all sectors except IPPU. This increase is dominated by Agriculture (+8%) and Waste (+6%).
824 For 2010-2018, the two main contributing regions for CH₄ emissions are Northern Africa and Sub-Saharan
825 Western Africa, Agriculture being the dominant emitting sector. From inversions, after withdrawing natural
826 emissions and wildfires using the GFED dataset from total CH₄ emissions, median values are almost always
827 below PRIMAP-hist estimates. CH₄ natural emissions have an important impact in Africa especially in the
828 Central African region as well as in the Southern countries. N₂O TD estimates are always higher than the ones
829 from PRIMAP-hist, underlining the importance to separate natural N₂O emissions from total estimates in order
830 to deliver appropriate anthropogenic assessments thanks to the inversions.

831 To compute a net budget for the three main GHG emissions and removals and for comparability we used the
832 MtCO₂e yr⁻¹ metric and latest IPCC report recommended GWP. The choice of a constructed GWP metric,
833 however, creates additional associated uncertainties notably due to the selected time horizon. By computing



834 the mean of methods excluding uncorrected UNFCCC and N₂O inversions data from twenty different ways for
835 assessing GHG emissions and removals in Africa, we found that the most recent net from the three main GHG
836 in Africa is a source of 2630_{1974}^{4557} MtCO₂e yr⁻¹.

837 Our assessment of African GHG emissions trends over 30 years through different methods can enable
838 comparisons of *ex post* with *ex ante* pledges of the PA, whose baseline year is often 1990. However, given the
839 global geopolitics to date featured with the prevailing principle of national sovereignty, a scientific assessment
840 of GHG can only work as a supporting tool (Janssens-Maenhout et al., 2020) and cannot be directly policy-
841 prescriptive. We note a relatively good match among the various types of estimates in terms of overall trends,
842 especially at a regional level and on a decadal basis, but large differences even among similar typologies of the
843 methods (TD or BU). The large discrepancies are a scientific limit to the possibility of precise verification of
844 the African country-reported emissions, but they are good enough to indicate trends. To compute a net from
845 the three main GHG, no purely “TD” method is available due to the necessity to replace N₂O inversions data
846 with BU data. An original result of this study is that we proposed at a small scale what may become a systematic
847 formalized methodological protocol for independent verification of a net estimate using country-reported data,
848 to be possibly implemented at the UNFCCC secretariat scale in a centralized way. The African GHG increasing
849 trend is not in line with the mitigation aims of the PA towards net-zero globally. Research teams focusing on
850 inversion methods (Nickless et al., 2020), underline that uncertainties should not be above 15% in order to
851 deliver a reasonable verification support capacity. A major source of complexity for the evaluation of the
852 respect of the Paris Agreement comes from the fact that national pledges generally fall below the discrepancies
853 between different scientific independent estimates. This calls for investments not only in improvements of
854 atmospheric measurement devices but also in the research efforts for standardizing verification methods. At
855 the policy level, the extrapolation of this study to the climate policy field could also serve as a compelling
856 argument for the creation of a global dedicated “Climate Inspection task force” of the UNFCCC.

857 **5 Data availability**

858 The datasets from the three main greenhouse gasses used in this paper (CO₂, CH₄, N₂O) from the various BU
859 inventories, TD inversions and DGVM over Africa will be made publicly available. This database is available
860 from Zenodo at: <https://doi.org/10.5281/zenodo.7347077> (Mostefaoui et al., 2022).

861 This dataset contains 32 data files:

862 - **CO₂ inversions** (annual flux for LULUCF CO₂)

863 - African CO₂ TD inversions GCB2020 1990-2019: annual CO₂ flux from GCB inversion models

864 - African CO₂ lateral flux 2001-2019: annual CO₂ lateral flux including river transport, crop and wood
865 product trade.

866 - African CO₂ TRENDYv9 1990-2019: annual CO₂ flux from 14 DGVM



867 - FAO 1990-2019: annual emissions and removals from FAO dataset
868 - Inventory IPCC 1990-2019: annual flux from inventory data collected from UNFCCC national
869 inventories in the IPCC categories
870 - **CH₄ inversions 2000-2017** (annual flux)
871 - African CH₄ global inversion 2000-2017: CH₄ flux over 2000-2017 from 11 in situ inversion and 11
872 satellite inversion models from four sectors; fossil refers to emissions from the fossil sector; agriculture and
873 waste refers to emissions from both the agriculture and waste sector; biomass burning refers to emissions from
874 biomass burning
875 - GFEDv4 1997-2016: wildfire emissions from the Global Fires Emission Dataset (GFED) version 4
876 - **N₂O inversions 1998-2017** (annual flux)
877 - N₂O PYVAR 1998-2017: total N₂O emissions from PyVAR inversions;
878 - N₂O TOMCAT-INVICAT 1998-2015: total N₂O emissions from TOMCAT-INVICAT model;
879 - N₂O MIROC4 - ACTM 1998-2016: total N₂O emissions from MIROC4-ACTM model;
880 Data used in this study are also included in the Supplementary Information (for example, from FAO data) and
881 on public websites (CDIAC, PRIMAP-hist, World Bank data). Any other data that support the findings of this
882 study are available from the corresponding author upon request.

883 **Author contributions.** MM, PC, PP and MJM designed research and led the discussions; MM wrote the initial
884 draft of the paper and edited all the following versions; MM made all figures ; MJM and PP processed the
885 original data from inversions and DGVM; MM processed the UNFCCC data and corrections; PC, PP and YE
886 gave valuable suggestions to the manuscript structure; PC, MJM and PPP read, gave comments and advice on
887 previous versions of the manuscript; all co-authors commented on specific parts related to their datasets; PC,
888 MJM, PP, FC, SS, CR, IL, MS, PP are data providers.

889 **Competing interests.** The authors declare that they have no conflict of interest.

890 **Disclaimer.** The views expressed in this publication are those of the authors.

891 **Acknowledgements**

892 MM acknowledges funding from Sorbonne University, Institute of the Environmental Transition. PC, PP, and
893 MJM were supported by the European Commission, Horizon 2020 Framework Program (VERIFY, grant no.
894 776810). PC and YE are also supported by the RECCAP2 project (grant no. ESRIN/4000123002/18/I-NB).
895 We acknowledge Stephen Sitch and Trendy modelers for the use of their dataset. We also acknowledge
896 Christian Rödenbeck for the use of CarboScope, Frédéric Chevallier for CAMS, Ingrid Luijkx for CTE,



897 Marielle Saunio for CH₄ inversions. The PyVAR-N₂O modeling results were provided by Rona Thompson
898 (NILU) and were funded through the Copernicus Atmosphere Monitoring Service
899 (<https://atmosphere.copernicus.eu/>), implemented by ECMWF on behalf of the European Commission, and
900 were generated using computing resources from LSCE.

901 **References**

- 902 Andrew, R. M.: A comparison of estimates of global carbon dioxide emissions from fossil carbon sources,
903 *Earth Syst. Sci. Data*, 12, 1437–1465, <https://doi.org/10.5194/essd-12-1437-2020>, 2020.
904
- 905 Ayompe, L. M., Davis, S. J., and Egoh, B. N.: Trends and drivers of African fossil fuel CO₂ emissions 1990–
906 2017, *Environ. Res. Lett.*, 15, 124039, <https://doi.org/10.1088/1748-9326/abc64f>, 2020.
907
- 908 BP. BP Statistical Review of World Energy, 2020.
909
- 910 Beck, H. E., Zimmermann, N. E., McVicar, T. R., Vergopolan, N., Berg, A., and Wood, E. F.: Present and
911 future Köppen-Geiger climate classification maps at 1-km resolution, *Sci. Data*, 5, 180214,
912 <https://doi.org/10.1038/sdata.2018.214>, 2018.
913
- 914 Bombelli, A., Henry, M., Castaldi, S., Adu-Bredu, S., Arneth, A., de Grandcourt, A., Grieco, E.,
915 Kutsch, W. L., Lehsten, V., Rasile, A., Reichstein, M., Tansey, K., Weber, U., and Valentini, R.:
916 An outlook on the Sub-Saharan Africa carbon balance, *Biogeosciences*, 6, 2193–2205,
917 <https://doi.org/10.5194/bg-6-2193-2009>, 2009.
918
- 919 Canadell, J. G., Raupach, M. R., and Houghton, R. A.: Anthropogenic CO₂ emissions in Africa,
920 *Biogeosciences*, 6, 463–468, <https://doi.org/10.5194/bg-6-463-2009>, 2009.
921
- 922 Chevallier, F., Fisher, M., Peylin, P., Serrar, S., Bousquet, P., Bréon, F.-M., Chédin, A., and Ciais, P.: Inferring
923 CO₂ sources and sinks from satellite observations: Method and application to TOVS data, *J. Geophys. Res.*
924 *Atmospheres*, 110, <https://doi.org/10.1029/2005JD006390>, 2005.
925
- 926 Ciais, P., Bastos, A., Chevallier, F., Lauerwald, R., Poulter, B., Canadell, J. G., Hugelius, G., Jackson, R. B.,
927 Jain, A., Jones, M., Kondo, M., Lujckx, I. T., Patra, P. K., Peters, W., Pongratz, J., Petrescu, A. M. R., Piao, S.,
928 Qiu, C., Von Randow, C., Regnier, P., Saunio, M., Scholes, R., Shvidenko, A., Tian, H., Yang, H., Wang, X.,
929 and Zheng, B.: Definitions and methods to estimate regional land carbon fluxes for the second phase of the
930 REgional Carbon Cycle Assessment and Processes Project (RECCAP-2), *Geosci. Model Dev.*, 15, 1289–1316,
931 <https://doi.org/10.5194/gmd-15-1289-2022>, 2022.
932
- 933 Deng, Z., Ciais, P., Tzompa-Sosa, Z. A., Saunio, M., Qiu, C., Tan, C., Sun, T., Ke, P., Cui, Y., Tanaka, K.,
934 Lin, X., Thompson, R. L., Tian, H., Yao, Y., Huang, Y., Lauerwald, R., Jain, A. K., Xu, X., Bastos, A., Sitch,
935 S., Palmer, P. I., Lauvaux, T., d’Aspremont, A., Giron, C., Benoit, A., Poulter, B., Chang, J., Petrescu, A. M.
936 R., Davis, S. J., Liu, Z., Grassi, G., Albergel, C., and Chevallier, F.: Comparing national greenhouse gas budgets
937 reported in UNFCCC inventories against atmospheric inversions, *Earth Syst. Sci. Data Discuss.*, 1–59,
938 <https://doi.org/10.5194/essd-2021-235>, 2021.
939
- 940 Dorfman, R.: A formula for the Gini Coefficient. *The Review of Economics and Statistics* Vol. 61, No. 1 ,
941 <https://doi.org/10.2307/1924845>, 1979.
942



- 943 FAOSTAT: available at: <https://www.fao.org/faostat/en/#data/GF>, last access: 3 May 2022.
944
- 945 FAO FRA: FAO Global Forests Resource Assessment, available at <fra-data.fao.org>, last access: June 2022,
946 2022.
947
- 948 Friedlingstein, P., Jones, M. W., O’Sullivan, M., Andrew, R. M., Hauck, J., Peters, G. P., Peters, W., Pongratz,
949 J., Sitch, S., Le Quéré, C., Bakker, D. C. E., Canadell, J. G., Ciais, P., Jackson, R. B., Anthoni, P., Barbero, L.,
950 Bastos, A., Bastrikov, V., Becker, M., Bopp, L., Buitenhuis, E., Chandra, N., Chevallier, F., Chini, L. P., Currie,
951 K. I., Feely, R. A., Gehlen, M., Gilfillan, D., Gkritzalis, T., Goll, D. S., Gruber, N., Gutekunst, S., Harris, I.,
952 Haverd, V., Houghton, R. A., Hurtt, G., Ilyina, T., Jain, A. K., Joetzjer, E., Kaplan, J. O., Kato, E., Klein
953 Goldewijk, K., Korsbakken, J. I., Landschützer, P., Lauvset, S. K., Lefèvre, N., Lenton, A., Lienert, S.,
954 Lombardozzi, D., Marland, G., McGuire, P. C., Melton, J. R., Metzl, N., Munro, D. R., Nabel, J. E. M. S.,
955 Nakaoka, S.-I., Neill, C., Omar, A. M., Ono, T., Peregon, A., Pierrot, D., Poulter, B., Rehder, G., Resplandy,
956 L., Robertson, E., Rödenbeck, C., Séférian, R., Schwinger, J., Smith, N., Tans, P. P., Tian, H., Tilbrook, B.,
957 Tubiello, F. N., van der Werf, G. R., Wiltshire, A. J., and Zaehle, S.: Global Carbon Budget 2019, *Earth Syst.*
958 *Sci. Data*, 11, 1783–1838, <https://doi.org/10.5194/essd-11-1783-2019>, 2019.
959
- 960 Friedlingstein, P., O’Sullivan, M., Jones, M. W., Andrew, R. M., Hauck, J., Olsen, A., Peters, G. P., Peters,
961 W., Pongratz, J., Sitch, S., Le Quéré, C., Canadell, J. G., Ciais, P., Jackson, R. B., Alin, S., Aragão, L. E. O.
962 C., Arneeth, A., Arora, V., Bates, N. R., Becker, M., Benoit-Cattin, A., Bittig, H. C., Bopp, L., Bultan, S.,
963 Chandra, N., Chevallier, F., Chini, L. P., Evans, W., Florentie, L., Forster, P. M., Gasser, T., Gehlen, M.,
964 Gilfillan, D., Gkritzalis, T., Gregor, L., Gruber, N., Harris, I., Hartung, K., Haverd, V., Houghton, R. A., Ilyina,
965 T., Jain, A. K., Joetzjer, E., Kadono, K., Kato, E., Kitidis, V., Korsbakken, J. I., Landschützer, P., Lefèvre, N.,
966 Lenton, A., Lienert, S., Liu, Z., Lombardozzi, D., Marland, G., Metzl, N., Munro, D. R., Nabel, J. E. M. S.,
967 Nakaoka, S.-I., Niwa, Y., O’Brien, K., Ono, T., Palmer, P. I., Pierrot, D., Poulter, B., Resplandy, L., Robertson,
968 E., Rödenbeck, C., Schwinger, J., Séférian, R., Skjelvan, I., Smith, A. J. P., Sutton, A. J., Tanhua, T., Tans, P.
969 P., Tian, H., Tilbrook, B., van der Werf, G., Vuichard, N., Walker, A. P., Wanninkhof, R., Watson, A. J., Willis,
970 D., Wiltshire, A. J., Yuan, W., Yue, X., and Zaehle, S.: Global Carbon Budget 2020, *Earth Syst. Sci. Data*, 12,
971 3269–3340, <https://doi.org/10.5194/essd-12-3269-2020>, 2020.
972
- 973 Gilfillan, D., and Marland G.: CDIAC-FF: global and national CO₂ emissions from fossil fuel combustion and
974 cement manufacture: 1751–2017, <https://doi.org/10.5194/essd-13-1667-2021>, 2021.
975
- 976 Grassi, G., House, J., Kurz, W. A., Cescatti, A., Houghton, R. A., Peters, G. P., Sanz, M. J., Viñas, R. A.,
977 Alkama, R., Arneeth, A., Bondeau, A., Dentener, F., Fader, M., Federici, S., Friedlingstein, P., Jain, A. K., Kato,
978 E., Koven, C. D., Lee, D., Nabel, J. E. M. S., Nassikas, A. A., Perugini, L., Rossi, S., Sitch, S., Viovy, N.,
979 Wiltshire, A., and Zaehle, S.: Reconciling global-model estimates and country reporting of anthropogenic forest
980 CO₂ sinks, *Nat. Clim. Change*, 8, 914–920, <https://doi.org/10.1038/s41558-018-0283-x>, 2018.
981
- 982 Grassi, G., Stehfest, E., Rogelj, J., van Vuuren, D., Cescatti, A., House, J., Nabuurs, G.-J., Rossi, S., Alkama,
983 R., Viñas, R. A., Calvin, K., Ceccherini, G., Federici, S., Fujimori, S., Gusti, M., Hasegawa, T., Havlik, P.,
984 Humpenöder, F., Korosuo, A., Perugini, L., Tubiello, F. N., and Popp, A.: Critical adjustment of land mitigation
985 pathways for assessing countries’ climate progress, *Nat. Clim. Change*, 11, 425–434,
986 <https://doi.org/10.1038/s41558-021-01033-6>, 2021.
987
- 988 Grassi, G., Conchedda, G., Federici, S., Abad Viñas, R., Korosuo, A., Melo, J., Rossi, S., Sandker, M.,
989 Somogyi, Z., and Tubiello, F. N.: Carbon fluxes from land 2000–2020: bringing clarity on countries’ reporting,
990 *Biogeosciences and biodiversity*, <https://doi.org/10.5194/essd-2022-104>, 2022.
991



- 992 Gütschow, J., Jeffery, M. L., Gieseke, R., Gebel, R., Stevens, D., Krapp, M., and Rocha, M.: The PRIMAP-
993 hist national historical emissions time series, *Earth Syst. Sci. Data*, 8, 571–603, [https://doi.org/10.5194/essd-8-](https://doi.org/10.5194/essd-8-571-2016)
994 571-2016, 2016.
- 995
996 Gütschow, J., Günther, A., Jeffery, M. L., and Gieseke, R.: The PRIMAP-hist national historical emissions
997 time series (1850-2018) v2.2, <https://doi.org/10.5281/zenodo.4479172>, 2021.
- 998
999 Houghton, R. A., House, J. I., Pongratz, J., van der Werf, G. R., DeFries, R. S., Hansen, M. C., Le Quéré, C.,
1000 and Ramankutty, N.: Carbon emissions from land use and land-cover change, *Biogeosciences*, 9, 5125–5142,
1001 <https://doi.org/10.5194/bg-9-5125-2012>, 2012.
- 1002
1003 IMF: International Monetary Fund: International Monetary Fund website, available at:
1004 <https://www.imf.org/en/Publications/fandd/issues/Series/Back-to-Basics/gross-domestic-product-GDP>, last
1005 access : February 2022.
- 1006
1007 IPCC: Good practice guidance for land use, land-use change and forestry /The Intergovernmental Panel on
1008 Climate Change. Edited by: Penman, J., Hayama, Kanagawa, 2006.
- 1009
1010 IPCC: Climate Change and Land: an IPCC special report on climate change, desertification, land degradation,
1011 sustainable land management, food security, and greenhouse gas fluxes in terrestrial ecosystems, [Shukla, P.R.,
1012 Skea, J., CalvoBuendia, E., Masson-Delmotte, V., Pörtner, H.-O., Roberts, D. C., Zhai, P., Slade, R., Connors,
1013 S., van Diemen, R., Ferrat, M., Haughey, E., Luz, S., Neogi, S., Pathak, M., Petzold, J., Portugal Pereira, J.,
1014 Vyas, P., Huntley, E., Kissick, K., Belkacemi, M., Malley, J. (eds.)]. In press, 2019.
- 1015
1016 IPCC: Revised 1996 IPCC Guidelines for National Greenhouse Inventories, IPCC/OECD/IEA, Paris, France,
1017 ISBN 92-64-15578-3, 1997.
- 1018
1019 IPCC: 2006 IPCC guidelines for National Greenhouse Gas Inventories, IGES, ISBN 4-88788-032-4, 2006.
- 1020
1021 IPCC: 2019 Refinement to the 2006 IPCC Guidelines for National Greenhouse Gas Inventories, edited by:
1022 Buendia, E., Tanabe, K., Kranjc, A., Baasansuren, J., Fukuda, M., Ngarize, S., Osako, A., Pyrozhenko, Y.,
1023 Shermanau, P., and Federici, S., Intergovernmental Panel on Climate Change (IPCC), Switzerland, ISBN 978-
1024 4-88788-232-4, 2019.
- 1025
1026 Janssens-Maenhout, G., Pinty, B., Dowell, M., Zunker, H., Andersson, E., Balsamo, G., Bézy, J.-L., Brunhes,
1027 T., Bösch, H., Bojkov, B., Brunner, D., Buchwitz, M., Crisp, D., Ciais, P., Counet, P., Dee, D., Gon, H. D. van
1028 der, Dolman, H., Drinkwater, M. R., Dubovik, O., Engelen, R., Fehr, T., Fernandez, V., Heimann, M.,
1029 Holmlund, K., Houweling, S., Husband, R., Juvyns, O., Kentarchos, A., Landgraf, J., Lang, R., Löscher, A.,
1030 Marshall, J., Meijer, Y., Nakajima, M., Palmer, P. I., Peylin, P., Rayner, P., Scholze, M., Sierk, B., Tamminen,
1031 J., and Veeffkind, P.: Toward an Operational Anthropogenic CO₂ Emissions Monitoring and Verification
1032 Support Capacity, *Bull. Am. Meteorol. Soc.*, 101, E1439–E1451, <https://doi.org/10.1175/BAMS-D-19-0017.1>,
1033 2020.
- 1034
1035 van der Laan-Luijckx, I. T., van der Velde, I. R., van der Veen, E., Tsuruta, A., Stanislawska, K.,
1036 Babenhauserheide, A., Zhang, H. F., Liu, Y., He, W., Chen, H., Masarie, K. A., Krol, M. C., and Peters, W.:
1037 The CarbonTracker Data Assimilation Shell (CTDAS) v1.0: implementation and global carbon balance 2001–
1038 2015, *Geosci. Model Dev.*, 10, 2785–2800, <https://doi.org/10.5194/gmd-10-2785-2017>, 2017.
- 1039
1040 Liousse, C., Assamoi, E., Criqui, P., Granier, C., and Rosset, R.: Explosive growth in African combustion
1041 emissions from 2005 to 2030, *Environ. Res. Lett.*, 9, 035003, <https://doi.org/10.1088/1748-9326/9/3/035003>,
1042 2014.



- 1043
1044 Mostefaoui, M., Ciais, P., McGrath, M. J., Peylin, P., Prabir, P. K., Saunois, M., Chevallier, F., Sitch, S.,
1045 Rodenbeck, C., Luijkx, I., and Thompson, R.: Datasets for greenhouse gasses emissions and removals from
1046 inventories and global models over Africa v0.1, Zenodo [data set], <https://doi.org/10.5281/zenodo.7347077>,
1047 2022.
1048
1049 Monks, S. A., Arnold, S. R., Hollaway, M. J., Pope, R. J., Wilson, C., Feng, W., Emmerson, K. M., Kerridge,
1050 B. J., Latter, B. L., Miles, G. M., Siddans, R., and Chipperfield, M. P.: The TOMCAT global chemical transport
1051 model v1.6: description of chemical mechanism and model evaluation, *Geosci. Model Dev.*, 10, 3025–3057,
1052 <https://doi.org/10.5194/gmd-10-3025-2017>, 2017.
1053
1054 Nickless, A., Scholes, R. J., Vermeulen, A., Beck, J., López-Ballesteros, A., Ardö, J., Karstens, U., Rigby, M.,
1055 Kasurinen, V., Pantazatou, K., Jorch, V., and Kutsch, W.: Greenhouse gas observation network design for
1056 Africa, *Tellus B Chem. Phys. Meteorol.*, 72, 1–30, <https://doi.org/10.1080/16000889.2020.1824486>, 2020.
1057
1058 Patra, P. K., Takigawa, M., Watanabe, S., Chandra, N., Ishijima, K., and Yamashita, Y.: Improved Chemical
1059 Tracer Simulation by MIROC4.0-based Atmospheric Chemistry-Transport Model (MIROC4-ACTM), *Sola*,
1060 14, 91–96, <https://doi.org/10.2151/sola.2018-016>, 2018.
1061
1062 Perugini, L., Pellis, G., Grassi, G., Ciais, P., Dolman, H., House, J. I., Peters, G. P., Smith, P., Günther, D., and
1063 Peylin, P.: Emerging reporting and verification needs under the Paris Agreement: How can the research
1064 community effectively contribute?, *Environ. Sci. Policy*, 122, 116–126,
1065 <https://doi.org/10.1016/j.envsci.2021.04.012>, 2021.
1066
1067 Petrescu, A. M. R., Qiu, C., Ciais, P., Thompson, R. L., Peylin, P., McGrath, M. J., Solazzo, E., Janssens-
1068 Maenhout, G., Tubiello, F. N., Bergamaschi, P., Brunner, D., Peters, G. P., Höglund-Isaksson, L., Regnier, P.,
1069 Lauerwald, R., Bastviken, D., Tsuruta, A., Winiwarter, W., Patra, P. K., Kuhnert, M., Oreggioni, G. D., Crippa,
1070 M., Saunois, M., Perugini, L., Markkanen, T., Aalto, T., Groot Zwaafink, C. D., Tian, H., Yao, Y., Wilson, C.,
1071 Conchedda, G., Günther, D., Leip, A., Smith, P., Haussaire, J.-M., Leppänen, A., Manning, A. J., McNorton,
1072 J., Brockmann, P., and Dolman, A. J.: The consolidated European synthesis of CH₄ and N₂O emissions for the
1073 European Union and United Kingdom: 1990–2017, *Earth Syst. Sci. Data*, 13, 2307–2362,
1074 <https://doi.org/10.5194/essd-13-2307-2021>, 2021.
1075
1076 PRIMAP-hist: PRIMAP-hist dataset, available at: <https://www.pik-potsdam.de/paris-reality-check/primap-hist>
1077 (last access: April 2022), 2021.
1078
1079 Rödenbeck, C.: Estimating CO₂ sources and sinks from atmospheric mixing ratio measurements using a global
1080 inversion of atmospheric transport, undefined, 2005.
1081
1082 Rodgers, C. D.: *Inverse Methods For Atmospheric Sounding: Theory And Practice*, World Scientific, 256 pp.,
1083 2000.
1084
1085 Saunois, M., Stavert, A. R., Poulter, B., Bousquet, P., Canadell, J. G., Jackson, R. B., Raymond, P. A.,
1086 Dlugokencky, E. J., Houweling, S., Patra, P. K., Ciais, P., Arora, V. K., Bastviken, D., Bergamaschi, P., Blake,
1087 D. R., Brailsford, G., Bruhwiler, L., Carlson, K. M., Carrol, M., Castaldi, S., Chandra, N., Crevoisier, C., Crill,
1088 P. M., Covey, K., Curry, C. L., Etiope, G., Frankenberg, C., Gedney, N., Hegglin, M. I., Höglund-Isaksson, L.,
1089 Hugelius, G., Ishizawa, M., Ito, A., Janssens-Maenhout, G., Jensen, K. M., Joos, F., Kleinen, T., Krummel, P.
1090 B., Langenfelds, R. L., Laruelle, G. G., Liu, L., Machida, T., Maksyutov, S., McDonald, K. C., McNorton, J.,
1091 Miller, P. A., Melton, J. R., Morino, I., Müller, J., Murguia-Flores, F., Naik, V., Niwa, Y., Noce, S., O’Doherty,
1092 S., Parker, R. J., Peng, C., Peng, S., Peters, G. P., Prigent, C., Prinn, R., Ramonet, M., Regnier, P., Riley, W.
1093 J., Rosentreter, J. A., Segers, A., Simpson, I. J., Shi, H., Smith, S. J., Steele, L. P., Thornton, B. F., Tian, H.,



- 1094 Tohjima, Y., Tubiello, F. N., Tsuruta, A., Viovy, N., Voulgarakis, A., Weber, T. S., van Weele, M., van der
1095 Werf, G. R., Weiss, R. F., Worthy, D., Wunch, D., Yin, Y., Yoshida, Y., Zhang, W., Zhang, Z., Zhao, Y.,
1096 Zheng, B., Zhu, Q., Zhu, Q., and Zhuang, Q.: The Global Methane Budget 2000–2017, *Earth Syst. Sci. Data*,
1097 12, 1561–1623, <https://doi.org/10.5194/essd-12-1561-2020>, 2020.
- 1098
1099 Sitch, S., Huntingford, C., Gedney, N., Levy, P. E., Lomas, M., Piao, S. L., Betts, R., Ciais, P., Cox, P.,
1100 Friedlingstein, P., Jones, C. D., Prentice, I. C., and Woodward, F. I.: Evaluation of the terrestrial carbon cycle,
1101 future plant geography and climate-carbon cycle feedbacks using five Dynamic Global Vegetation Models
1102 (DGVMs), *Glob. Change Biol.*, 14, 2015–2039, <https://doi.org/10.1111/j.1365-2486.2008.01626.x>, 2008.
- 1103
1104 Thompson, R. L., Chevallier, F., Crotwell, A. M., Dutton, G., Langenfelds, R. L., Prinn, R. G., Weiss, R. F.,
1105 Tohjima, Y., Nakazawa, T., Krummel, P. B., Steele, L. P., Fraser, P., O’Doherty, S., Ishijima, K., and Aoki,
1106 S.: Nitrous oxide emissions 1999 to 2009 from a global atmospheric inversion, *Atmospheric Chem. Phys.*, 14,
1107 1801–1817, <https://doi.org/10.5194/acp-14-1801-2014>, 2014.
- 1108
1109 Tian, H., Xu, R., Canadell, J. G., Thompson, R. L., Winiwarter, W., Suntharalingam, P., Davidson, E. A., Ciais,
1110 P., Jackson, R. B., Janssens-Maenhout, G., Prather, M. J., Regnier, P., Pan, N., Pan, S., Peters, G. P., Shi, H.,
1111 Tubiello, F. N., Zaehle, S., Zhou, F., Arneth, A., Battaglia, G., Berthet, S., Bopp, L., Bouwman, A. F.,
1112 Buitenhuis, E. T., Chang, J., Chipperfield, M. P., Dangal, S. R. S., Dlugokencky, E., Elkins, J. W., Eyre, B. D.,
1113 Fu, B., Hall, B., Ito, A., Joos, F., Krummel, P. B., Landolfi, A., Laruelle, G. G., Lauerwald, R., Li, W., Lienert,
1114 S., Maavara, T., MacLeod, M., Millet, D. B., Olin, S., Patra, P. K., Prinn, R. G., Raymond, P. A., Ruiz, D. J.,
1115 van der Werf, G. R., Vuichard, N., Wang, J., Weiss, R. F., Wells, K. C., Wilson, C., Yang, J., and Yao, Y.: A
1116 comprehensive quantification of global nitrous oxide sources and sinks, *Nature*, 586, 248–256,
1117 <https://doi.org/10.1038/s41586-020-2780-0>, 2020.
- 1118
1119 Tongwane, M. I. and Moeletsi, M. E.: A review of greenhouse gas emissions from the agriculture sector in
1120 Africa, *Agric. Syst.*, 166, 124–134, <https://doi.org/10.1016/j.agry.2018.08.011>, 2018.
- 1121 UNFCCC: UNFCCC: National Inventory Submissions, available at: <https://unfccc.int/> (last access : March
1122 2021), 2021.
- 1123
1124 UNFCCC REDD+: REDD+ National Reports, available at: <https://redd.unfccc.int/submissions.html?topic=6>
1125 (last access: July 2022), 2022.
- 1126 United Nations Department of Economic and Social Affairs, Population Division: World Population Prospects
1127 2019: Summary of Results, 2019.
- 1128
1129 Valentini, R., Arneth, A., Bombelli, A., Castaldi, S., Cazzolla Gatti, R., Chevallier, F., Ciais, P., Grieco, E.,
1130 Hartmann, J., Henry, M., Houghton, R. A., Jung, M., Kutsch, W. L., Malhi, Y., Mayorga, E., Merbold, L.,
1131 Murray-Tortarolo, G., Papale, D., Peylin, P., Poulter, B., Raymond, P. A., Santini, M., Sitch, S., Vaglio Laurin,
1132 G., van der Werf, G. R., Williams, C. A., and Scholes, R. J.: A full greenhouse gases budget of Africa: synthesis,
1133 uncertainties, and vulnerabilities, *Biogeosciences*, 11, 381–407, <https://doi.org/10.5194/bg-11-381-2014>, 2014.
- 1134
1135 van der Werf, G. R., Randerson, J. T., Giglio, L., van Leeuwen, T. T., Chen, Y., Rogers, B. M., Mu, M., van
1136 Marle, M. J. E., Morton, D. C., Collatz, G. J., Yokelson, R. J., and Kasibhatla, P. S.: Global fire emissions
1137 estimates during 1997–2016, *Earth Syst. Sci. Data*, 9, 697–720, <https://doi.org/10.5194/essd-9-697-2017>, 2017.
- 1138
1139 Wilson, C., Chipperfield, M. P., Gloor, M., and Chevallier, F.: Development of a variational flux inversion
1140 system (INVICAT v1.0) using the TOMCAT chemical transport model, *Geosci. Model Dev.*, 7, 2485–2500,
1141 <https://doi.org/10.5194/gmd-7-2485-2014>, 2014.
- 1142
1143 World Bank: GDP exchange rate estimates, available at
1144 <https://data.worldbank.org/indicator/NY.GDP.MKTP.CD> last accessed, 2019.



- 1145
1146 World Bank: World Bank economic data, available at: <https://www.worldbank.org/> (last access: May 2022),
1147 2022.
1148
1149 Zhu, Y., Merbold, L., Pelster, D., Diaz-Pines, E., Wanyama, G. N., and Butterbach-Bahl, K.: Effect of Dung
1150 Quantity and Quality on Greenhouse Gas Fluxes From Tropical Pastures in Kenya, *Glob. Biogeochem. Cycles*,
1151 32, 1589–1604, <https://doi.org/10.1029/2018GB005949>, 2018.
- 1152 van der Zwaan, B., Kober, T., Longa, F. D., van der Laan, A., and Jan Kramer, G.: An integrated assessment
1153 of pathways for low-carbon development in Africa, *Energy Policy*, 117, 387–395,
1154 <https://doi.org/10.1016/j.enpol.2018.03.017>, 2018.